SULPHATION OF CUPROUS AND CUPRIC OXIDE DUSTS AND HETEROGENEOUS COPPER MATTE PARTICLES IN SIMULATED FLASH SMELTING HEAT RECOVERY BOILER CONDITIONS

Tiina Ranki-Kilpinen

Dissertation for the degree of Doctor of Science in Technolgy to be presented with due permission of the Department of Materials Science and Rock Engineering for public examination and debate in Auditorium V1 at Helsinki University of Technology (Espoo, Finland) on the 28th of April, 2004, at 12 o'clock noon.

ABSTRACT

Copper smelting with the Outokumpu flash smelting process generates significant amounts of SO_2-rich off-gas and flue dust. From the smelting unit, gases with a dust load are directed into a heat recovery boiler (also known as a waste heat boiler). In the radiation section temperature decreases, sulphates become thermodynamically stable, and the sulphation of oxidic dust particles commences. Releasing heat may lead to an increase in particle temperatures, softening of the sulphated particles, and the formation of dust accretions on the heat transfer surfaces. Decreased heat transfer efficiency and blockages of the gas flow paths may cause severe operational problems. To maintain stable boiler operation, sulphation behaviour has to be well understood, but only scant published data concerning dust sulphation reactions is available. The objective of this work was to gain basic knowledge of the sulphation behaviour of dust components to ascertain that boiler design and operation can be carried out so that sulphate formation takes place in a controlled manner.

The reactions of synthetic Cu_2O and CuO (mainly 37-53 µm) and a partially oxidised copper matte were studied experimentally with the aim of arriving at a better understanding of dust sulphation in industrial heat recovery boilers. The parameters in the laboratory-scale experiments were gas composition (20-60 vol-% SO_2, 2.5-10 vol-% O_2), temperature (560-660°C), reaction time, and particle size. Standard chemical analysis and scanning electron microscopy with EDS were utilised when examining the samples.

Sulphate formation was found to be sensitive to gas composition and temperature. Also particle size and surface morphology have significant effects on the sulphation rate. On the basis of the experimental results the temperature range for effective sulphation of pure cuprous oxide is narrow; the optimal sulphate formation temperature lies between 580-640°C, depending on the gas composition. An increase in oxygen concentration expands the favourable temperature range and lowers the most optimal sulphate formation temperature; on the contrary an increase in sulphur dioxide concentration raises the favourable sulphation temperature.

On the basis of the present experiments pure cupric oxide behaves like cuprous oxide, but the conversion degrees are slightly lower and there is not such a clear enhance in the sulphation rate at a certain temperature.

Fine, heterogeneous partially oxidised matte reacts significantly faster compared to synthetic oxides. The reason for more effective sulphation is suggested to be the smaller particle size and more detailed morphology (larger specific surface area).

In the heat recovery boiler dust particles must have a sufficient residence time in the gas phase at a correct temperature range to allow the dust particles to reach complete conversion in the radiation section before they enter the boiler convection section and come into contact with the convection tube banks. Enough oxygen has to be supplied to the appropriate zone to ensure effective sulphation at the right place. Also, mixing of the oxygen must be efficient.

PREFACE

The experimental research work of this thesis was carried out in the Laboratory of Materials Processing and Powder Metallurgy, Helsinki University of Technology, during the years 1998-2002.

Espoo, 08.10.2003

Tiina Ranki-Kilpinen

TABLE OF CONTENTS

1 INTRODUCTION

1.1 Flue dust in flash smelting off-gas line

The pyrometallurgical processing of copper and nickel sulphides involves smelting and refining operations at high temperatures. Today Outokumpu Flash Smelting *[Bry58]* is a dominant technology for primary copper production (Fig.1). The process involves the oxidation of dried feed concentrates, fluxes, and re-cycled dust in a suspension high in oxygen and temperature. Process outputs are matte, slag, and significant amounts of off-gas rich in sulphur dioxide (20-70 vol-%), and oxidic flue dust (approximately 4-10% of solid feed). Off-gases with a dust load leave the flash smelting furnace at 1200 to 1400°C and are directed through gas treatment facilities (heat recovery boiler, electrostatic precipitator), where the gas is cooled and the dust particles are captured. Because of the high copper content, approximately 30 wt-% Cu (and environmental aspects), dust is re-cycled back to the process. *[Han98/Kyt97 /Bis94]*
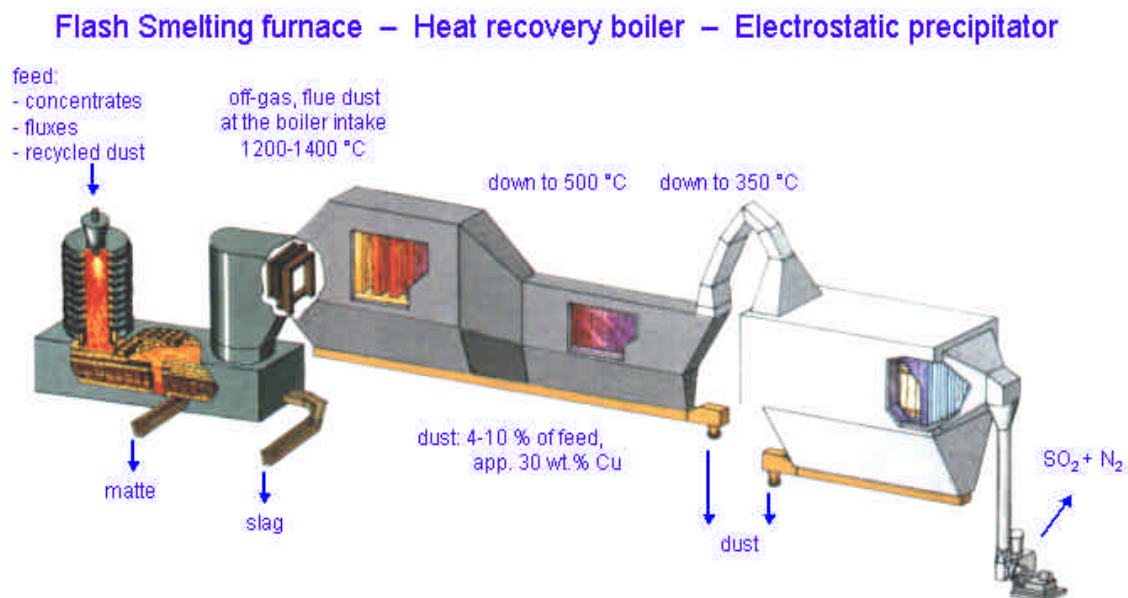
Figure 1. Outokumpu Flash Smelting process; flash smelting furnace, heat recovery boiler, and electrostatic precipitator

Flue dust is composed of mechanically formed solid/liquid particles which do not settle down in the flash smelting furnace but follow the process gas, and compounds/species (Cu, impurities), which have been vapourised in the burning zone of the process and condensed from the process gas at lower temperatures, i.e. chemically formed dust. Generally, the dust is heterogeneous and small in size, 10-20 µm, compared to feed concentrate. *[Sam01a/Kyt97/Yan96]*

In the furnace off-take sulphidic dust may stick to the walls of the boiler throat, forming hard accretions. Air/oxygen injection to the uptake shaft can be applied to oxidise the matte, i.e. the rest of the sulphides, to non-sticky oxides. Thus, the flue dust entering the heat recovery boiler is mainly in oxide form. An average particle size is 10-20 µm, and the residence time of a single particle in the boiler is typically 15-30 seconds. *[Swi02/Kyt97/Yan96]*

In the radiation part the temperature cools down to 700-500°C and metallic sulphates become thermodynamically stable. As all the required reactants are formed as by-products in the process, the sulphation of oxidic flue-dust inevitably commences *[Kyt97/Yan96]*. Reactions are highly exothermic. Releasing heat causes an increase in particle temperatures and softening of the particles. When sulphated particles are close to their sintering temperature they may stick to the heat transfer surfaces (radiation sheets, convection tubes) of the boiler.

Dust accretion causes severe operational problems, such as reduced heat transfer efficiency, which leads to higher boiler outlet temperatures, and blockages of the gas flow paths. Because of the build-ups boiler needs to be continuously rapped, which stresses the steam tubes of the boiler. Thus, the boiler must facilitate the cooling and freezing of the molten particles so that they do not agglomerate on the boiler walls. It is desirable that sulphate formation should take place in the radiation section, in the gas phase, before the particles come into contact with the boiler walls or enter the convection section. The amount of sulphation air (oxygen) must also be correct. Too small an amount leads to incomplete sulphation, and sulphidic compounds stick to the boiler surfaces even more tightly than sulphates. On the other hand, excess oxygen increases the formation of corrosive weak acid. Flue dust formation is considered to be characteristic for smelting processes like the flash smelting, Mitsubishi, Isasmelt, etc. Thus, the dust build-up problems are not limited to Outokumpu flash smelting process gas handling equipment but concern also flash converting as well as other metallurgical processes. *[Swi02/Bis94/Dav87/Jon96/Saf98 /StE94/Liu03]*

1.2 Motive for the thesis

Fundamental knowledge of flue dust behaviour in heat recovery boiler conditions is still inadequate. The sulphation of copper oxides has been intensively studied thermogravimetrically, using pellets and powders in crucibles, and also with different kinds of fluid-bed systems. However, the focus has been on roasting process conditions, and thus the particle diameters of interest have been measured in millimetres instead of micrometers and sulphation times in hours rather than seconds *[Wad60/Hoc66/Sah84-85]*. The objective of this thesis is to improve the basic knowledge of dust sulphation behaviour and in that way help to improve the operation and control of the off-gas line.

Research concentrating on dust sulphation started at the Helsinki University of Technology in 1997. A laboratory-scale fluid-bed reactor was constructed to experimentally study sulphation phenomena in simulated boiler conditions, find optimal conditions for effective sulphate formation and gain basic knowledge of the sulphation behaviour of typical dust components *[Ran00]*. Work was started with pure cuprous and cupric oxide *[Ran00/Peu01/Ran02]* and continued with partly oxidised copper matte. This information is required in order to ascertain that boiler design and operation can be carried out so that sulphate formation takes place in a controlled manner. The results of this study may also serve as verification data for numerical boiler simulations.

2 EXPERIMENTAL

2.1 Equipment

A laboratory-scale fluid-bed furnace was designed and constructed in order to experimentally simulate sulphation phenomena in the industrial heat recovery boiler. The design details (e.g. dimensions, gas flow rates, material feeding, etc.,) were first tested with a couple of 'cold models'. In the furnace particles are in loose contact with each other, which creates ideal reaction conditions. The experimental temperature, gas composition, and reaction time can be adjusted to correspond to the boiler conditions.

A schematic illustration of the reactor unit and applied conditions is presented in Fig. 2. The reactor is shaped from transparent quartz glass. A removable sintered quartz grid (porosity grade 0) divides the tube into the reaction zone and gas heating zone, which is filled with alumina pearls to improve heat transfer and gas mixing. The diameter of the reaction zone is 33 mm and the height of the vertical reaction zone 20 mm, after which the tube starts widening in order to slow down the gas flow rate and prevent particles escaping to the off-gas line. An inclined feeder tube is used to direct solid particles to the reaction zone.

Two semicylinders (Kanthal HAS 200) form the reactor heating system. Their heating is adjusted by a Honeywell-made temperature controller using an S-type thermocouple (Pt-Pt/10%Rh). The heating elements are hinged, and parts can be opened to facilitate visual observation of the hovering particles.

Gas flows are monitored by rotameters together with electrically-operated valves so as to obtain quick shifts between inert purging gas (N_2 industrial grade 99.5%) and reaction gas (bottled pure SO_2 and O_2-N_2 mixtures) flows. The off-gas is neutralised by a 10% NaOH solution using a counter-flow-type scrubber. All the gases were supplied by Oy Aga Ab.

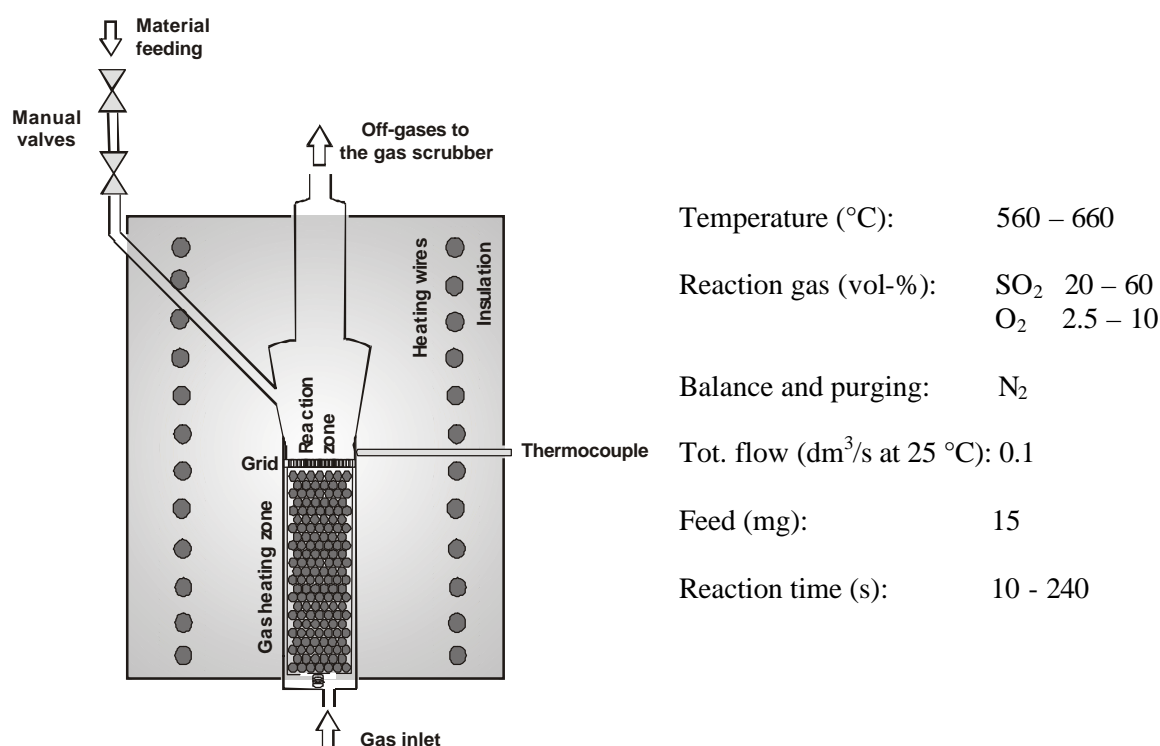|	
Temperature (°C):	560 – 660
Reaction gas (vol-%):	SO_2 20 – 60
	O_2 2.5 – 10
Balance and purging:	N_2
Tot. flow (dm^3/s at 25 °C):	0.1
Feed (mg):	15
Reaction time (s):	10 - 240

Figure 2. Schematic picture of fluid-bed reactor and parameters in the experiments

2.2 Experimental procedure

In an experiment, 1.5 grams of screened solid reactant and a total gas flow of 0.1 dm^3/s (~0.4 m/s at 600°C at 1 atm in the reaction zone) were used. The amount of powder was enough for both chemical analysis and sample preparation for microscopical studies, but studied so as not to be a rate-controlling factor. The flow rate was adjusted empirically to be just enough to maintain fluidisation. The weighted amount of screened oxide particles was directed to the reaction zone, into an inert nitrogen flow, which was introduced into the reaction chamber via the heating section. When the particles reached the experimental temperature the inert gas was replaced by the reaction gas mixture. When the desired reaction time had passed, the reaction gas was changed back to the nitrogen flow again. After purging, the reacted sample was removed from the grid and placed into an exsiccator.

2.3 Analytical methods

The chemical analysis of all the samples was carried out at the Analytical Laboratory of Outokumpu Research Oy (Pori, Finland). Sulphur (S) was determined using a Leco analyser (Model CS 244). The amount of sulphate (SO$_4$) was analysed using an ionchromatograph (IC). For non-synthetic samples, Fe and Cu analyses were performed using standard ICP techniques.

To characterise the feed materials, a Malvern particle size analyser (Mastersizer 2000) with a Hydro 2000SM sample dispersion unit was used to measure the volumetric particle size distribution of the feeds.

The specific surface areas of the feed fractions were measured using BET-method at the Analytical Laboratory of Outokumpu Research Oy (Pori, Finland).

Microscopic examinations were carried out using a scanning electron microscope (SEM), LEO 1450 by LEO Electron Microscopy Ltd, which was equipped with an energy dispersive spectrometer (EDS), supplied by Link Nordiska AB, for elemental analysis. Morphology was visually studied from secondary electron (SE) images. The internal structures (product layers) of the samples were examined from cross-sections, using a backscatter electron detector. The EDS was used for element mapping and point analysis.

2.4 Characterisation of raw materials

Three different materials were studied. Although industrial process dust is heterogeneous, synthetic pure oxides were chosen first for the research programme in order to enable the identification of the influences of different parameters. Experiments were started with synthetic cuprous oxide (Cu$_2$O) powder, and continued with pure cupric oxide (CuO). Feeds were selected on the basis of the prevailing sulphate-forming components of the dust entering the HRB. The synthetic powders were prepared by Outokumpu Research Oy in Pori, Finland. In addition to pure, homogeneous oxides, a few series of experiments were conducted with a non-synthetic oxide-sulphide mixture. This raw material was prepared by oxidising low-iron copper matte (Cu 64.8, Fe 6.0, S 21.0 wt-%) in the laminar flow furnace *[Peu00]*. Oxidation behaviour of such copper mattes with low iron content has been intensively studied at the Helsinki University of Technology. *[Peu99]*

2.4.1 Cuprous oxide

For synthetic Cu_2O 2 mm-thick Outokumpu HCOF (99.999% Cu) copper plates were oxidised at 1050°C in an air atmosphere for a week, until the metallic heart disappeared. The treatment was followed by homogenisation of the extra oxygen in an N_2 atmosphere at 950°C for a day. The Cu_2O that was formed was crushed and sieved [Tas02]. Mainly, a screen fraction of 37–53 µm was used in the experiments.

The measured volumetric particle size distribution of the cuprous oxide fraction used is presented in Fig. 3. On the basis of the measurements, the average particle diameter is 48 µm, 10 vol-% being below 26 µm and 90 vol-% below 78 µm.
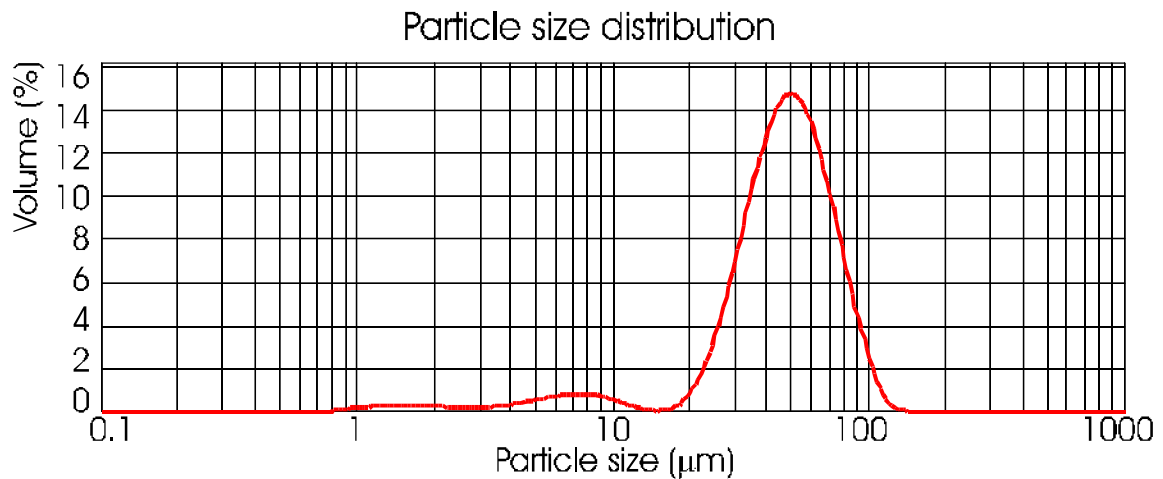
Figure 3. Volumetric particle size distribution of Cu$_2$O, nominal screen fraction 37–53 µm

The morphology micrographs of the original Cu_2O are presented in Fig. 4. The particles are irregular and oblong, which explains why size distribution analysis gives slightly larger particle sizes than the sieve sizes used indicate. The edges of the particles are sharp, as they are crushed. Tiny dust particles, originating from crushing, stand on the flat particle surfaces. Surface porosity is negligible.
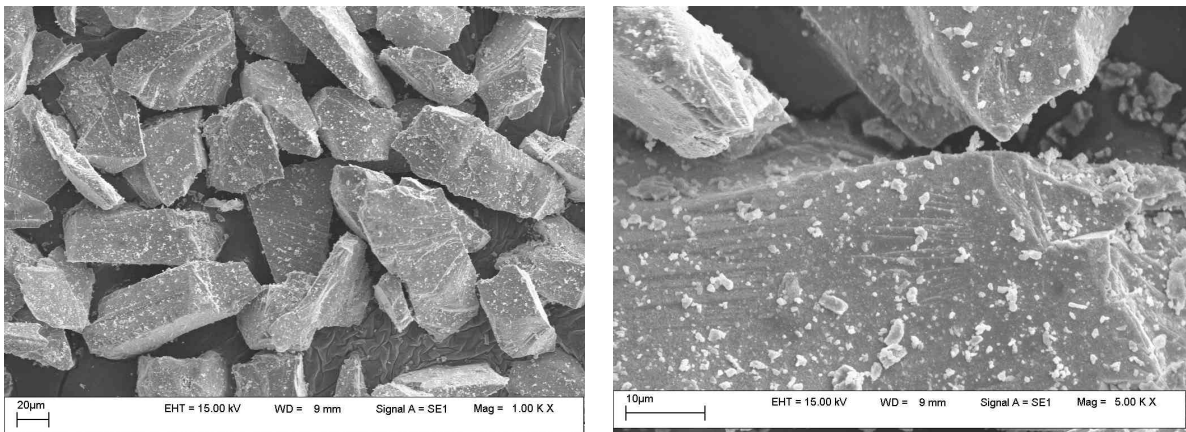
Figure 4. An overview and a detailed picture of the pure Cu$_2$O, nominal screen fraction 37–53 µm

A series of experiments was also conducted with sub-micron-sized cuprous oxide (Fig. 5). The powder was prepared by precipitation with NaOH from a concentrated

Cu$^+$/NaCl solution and stored in water *[Tas02]*. Before the experiments the powder was dried at 60°C in an N$_2$ atmosphere. The powder appeared to agglomerate significantly. The free surface area is still notably larger, compared to coarser synthetic oxide.
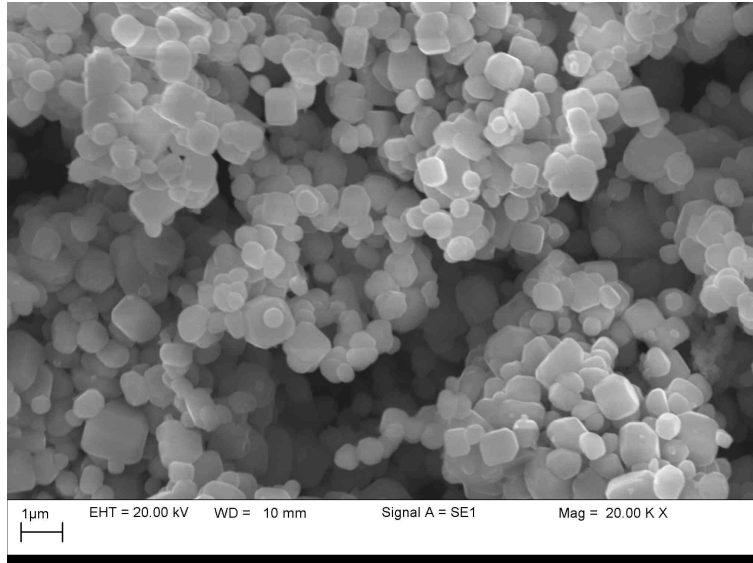
Figure 5. An overview of pure sub-micron-sized cuprous oxide

2.4.2 Cupric oxide

Synthetic CuO was prepared by oxidising Cu plate at 950°C for a week and then treating it at 700°C in air for another week *[Tas02]*. The same screen fraction of 37–53 µm was used in the experiments. On the basis of the size distribution measurements (Fig. 6.), the average particle diameter is 49 µm, 10 vol-% being below 25 µm and 90 vol-% below 83 µm. Morphology images of the CuO are presented in Fig. 7. The surface structure seems to be identical with that of the Cu$_2$O used.
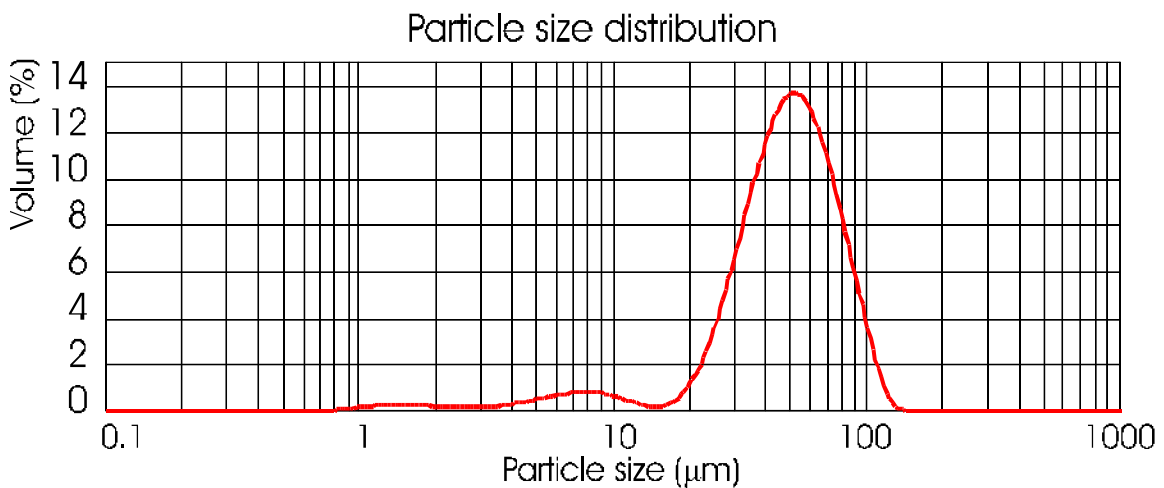

Figure 6. Volumetric particle size distribution of CuO, nominal screen fraction 37–53 µm
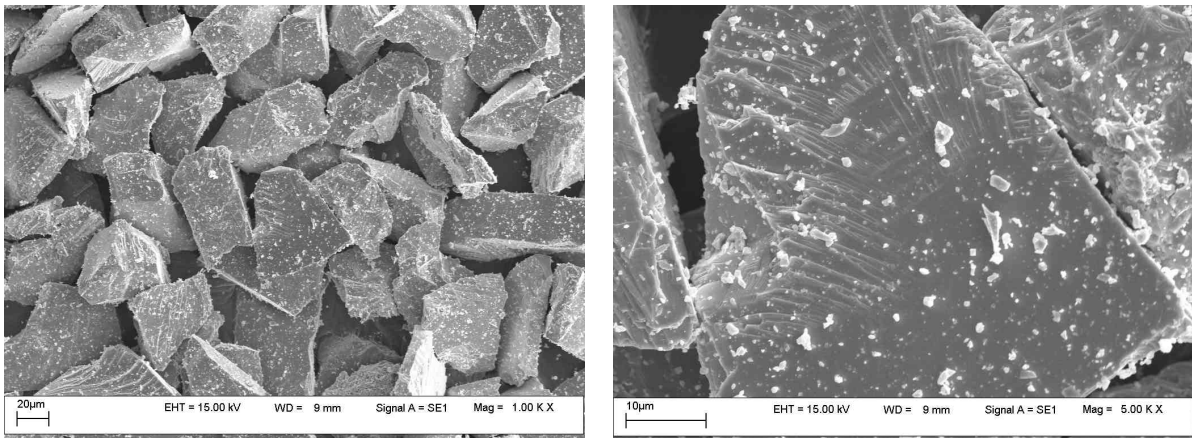
Figure 7. An overview and closer look at the pure CuO, nominal screen fraction 37–53 µm

2.4.3 Partially oxidised Cu matte

The screen fraction of 40-75 µm of copper matte was incompletely oxidised in the laminar flow furnace, which had been used earlier for several oxidation behaviour studies of copper and nickel concentrates and mattes *[Peu00]*. The chemical composition after oxidation at 1000°C in an air atmosphere was 67.9 wt-% Cu, 8.0 wt-% Fe, and 6.7 wt-% S. Approximately 30 wt-% of the original sulphur was still left in the powder. The prepared material roughly corresponds to industrial flue dust. Particle size was significantly reduced during the oxidation, due to the fragmentation. The average particle diameter of the product was measured to be 10 µm, 10 vol-% being below 2 µm and 90 vol-% below 55 µm (Fig. 8).

Unlike the synthetic feeds, this powder was not homogeneous. On the basis of the microscopic observations and element analysis, there were few larger particles (+20 µm) with copper sulphide cores surrounded by iron/copper oxide shells and a large amount of smaller (-10 µm) sulphidic and oxidic particles. Overviews and higher magnifications of typical small particles are shown in Fig. 9.

Figure 8. Volumetric particle size distribution of the partially oxidised matte

a) General view

b) Sulphidic (white) and oxidic particles

c) Morphology of the small particles

d) Dense (sulphidic) particles, porous (oxidic) particles
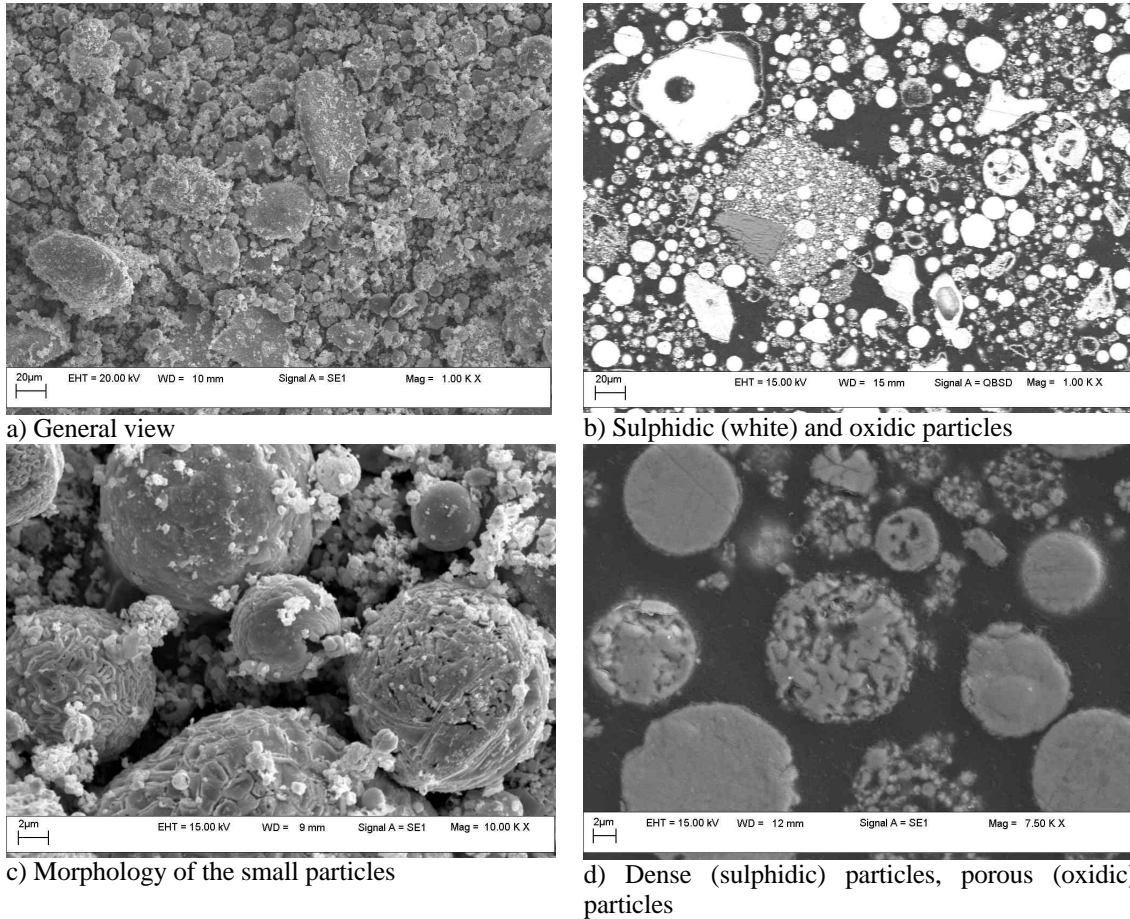
Figure 9. Morphology and internal structure of the partially oxidised copper matte

2.4.4 Specific surface areas
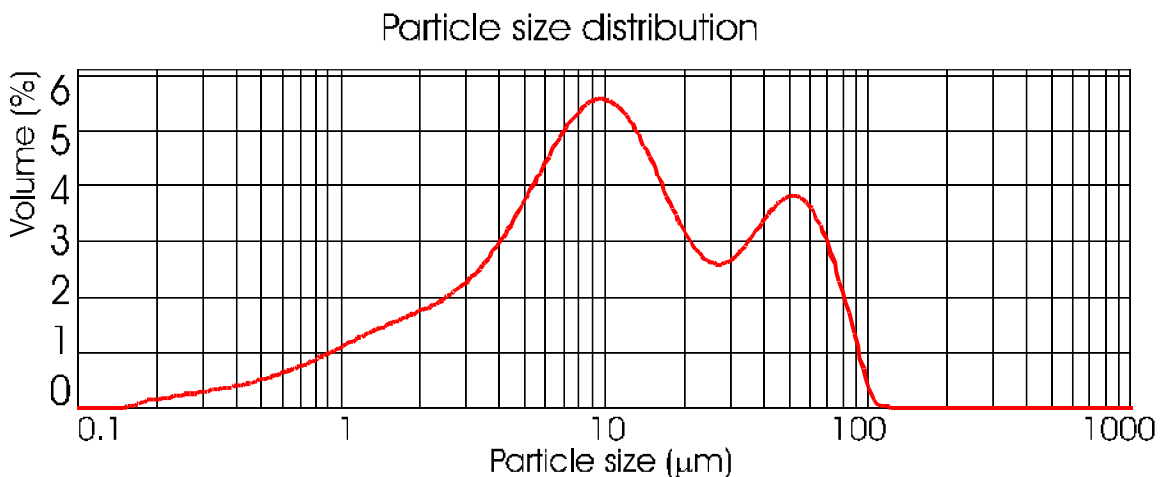
In idealised case where particles are cubes of equal size with an edge of *l* and density of solid r the specific surface area *S* (the area exposed by one gram of particles) is defined by the following expression: *[Gre67, Low91]*

$$S = \frac{6}{rl} \qquad (1).$$

If the edge *l* is 1 µm, and r is 6 g/cm^3 (density of Cu_2O according to HSC-database), the theoretical specific surface area is 1 m^2/g. Because of the surface imperfections (roughness, porosity) real surface areas are always greater than the theoretical area. *[Low91]* In practice the (fine) particles may stick together and form agglomerates, when the surface area is lost. *[Gre67]*

Measured specific surface areas of the studied feed materials and a theoretically calculated minimum area are presented in Fig. 10. In general, specific surface areas increase with decreasing particle size. Cupric oxide seems to have slightly smaller specific surface area than cuprous oxide. However, on the basis of these few analysis definite conclusions cannot be made. Measured specific surface area of the sub-micron-sized cuprous oxide corresponds to the theoretical minimum area. Due to the significant agglomeration the available surface area might be even smaller. The partially oxidised Cu matte has the largest specific surface area of the used materials.
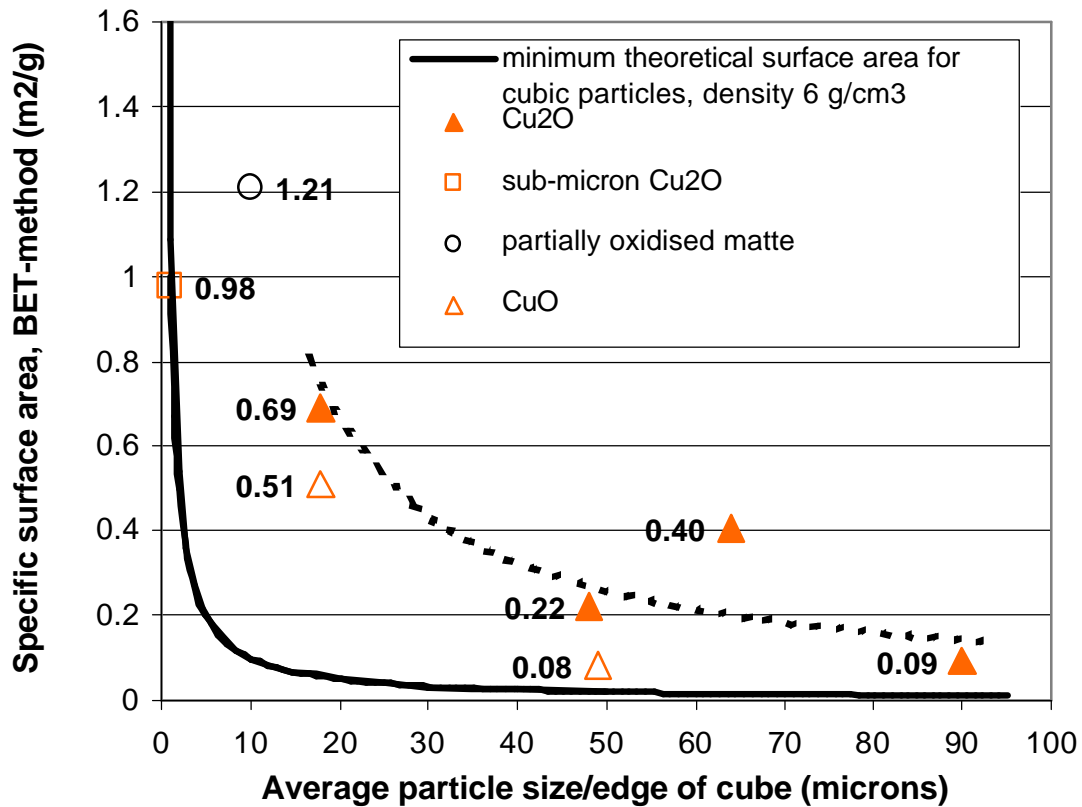
Figure 10. Measured specific surface areas of studied feed materials and calculated theoretical specific surface area for cubic particles with the density of 6 g/cm³.

2.5 Preliminary experiments

The equipment was first tested with cuprous oxide, with a screen fraction of 74–105 µm *[Ran00]*. Such a coarse fraction was chosen for the preliminary experiments to facilitate the experiments, sample preparation and SEM-studies. On the basis of the results, some modifications and changes were made both to the equipment and experimental procedure *[Peu01]*. In addition to structural changes, the particle feed amount was reduced and gas flow rate increased. A few series of the preliminary results are presented in Fig. 11. The optimal temperature area for sulphate formation seemed to be between 600-650°C; at 700°C sulphate formation was negligible. The conditions (temperature range) for the current experiments were selected on the basis of the results of these preliminary tests.

Figure 11. Preliminary experiments; 20 vol-% SO₂, 40 vol-% O₂, nominal size fraction 74–105 μm, feed amount 30 mg, gas flow rate 0.083 dm³/s, residence times 60, 80 and 120 s.

3 RESULTS

The results of the chemical analyses are converted to sulphation curves and surfaces and presented in the following chapters. Actual data points and fitted curves are presented in two-dimensional graphs; 3D surfaces are formed out of fitted curves and used only to illustrate the sulphation behaviour trends and effects of applied parameters.

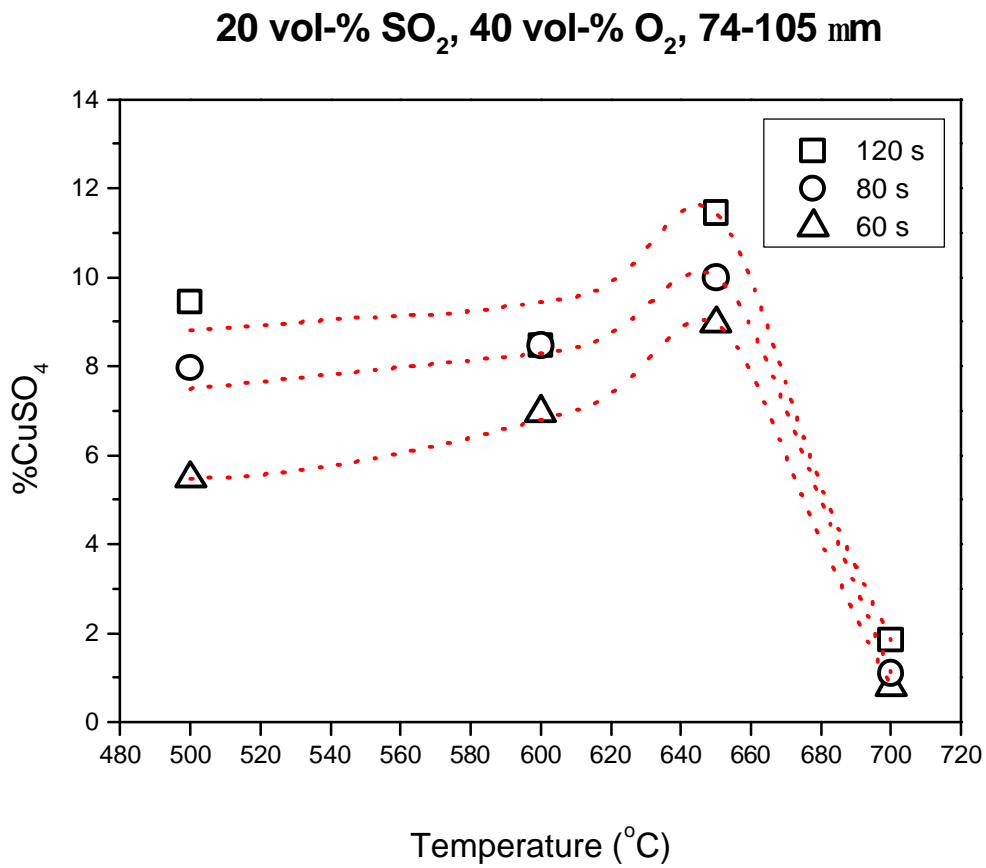In the case of an industrial heat recovery boiler the degree of sulphation is often defined as the ratio of sulphur as SO_4 compared to all sulphur analysed (sulphation degree of sulphur). Another applied method is to compare copper in sulphate form to the total copper in dust (sulphation degree of copper).

Here the Cu_2O and CuO were pure oxides, totally free of sulphur, thus comparison of sulphur in sulphate form versus total sulphur is not appropriate. The results of the Cu_2O and CuO experiments are presented as weight percentages of copper sulphate ($CuSO_4$) in the samples calculated based on sulphur (S) or sulphate (SO_4) analysis, and based on an average of the analysis, when both are available. Here sulphation degree is defined as:

$$\%CuSO_4 = \%S \cdot \frac{M_{CuSO_4}}{M_S} = \%SO_4 \cdot \frac{M_{CuSO_4}}{M_{SO_4}} \tag{2}.$$

When comparing the separate S and SO_4 analysis of the same reacted synthetic oxide samples, elemental sulphur almost matches the sulphur in SO_4, meaning that practically all the sulphur in the synthetic samples is in sulphate form. Deviations in the amounts of sulphate calculated on the basis of different analyses are small and of a random nature.

The results of the matte experiments and comparison of all the results are presented directly as $\%SO_4$ analysed in the samples, since, in addition to copper sulphate, the co-existence of iron sulphate is probable in matte samples. The chemical analyses are collected in Appendix A.

3.1 Sulphation of synthetic Cu₂O

As can be noticed from the phase stability diagram presented in Fig. 12, the stable copper oxide in the copper smelting conditions at the heat recovery boiler inlet is Cu_2O. Thus, the experiments were started with it. Sulphate formation is highly dependent on the prevailing temperature and gas composition. The effects of the experimental temperature, reaction gas composition, residence time, particle size, and Pt catalyst were studied.
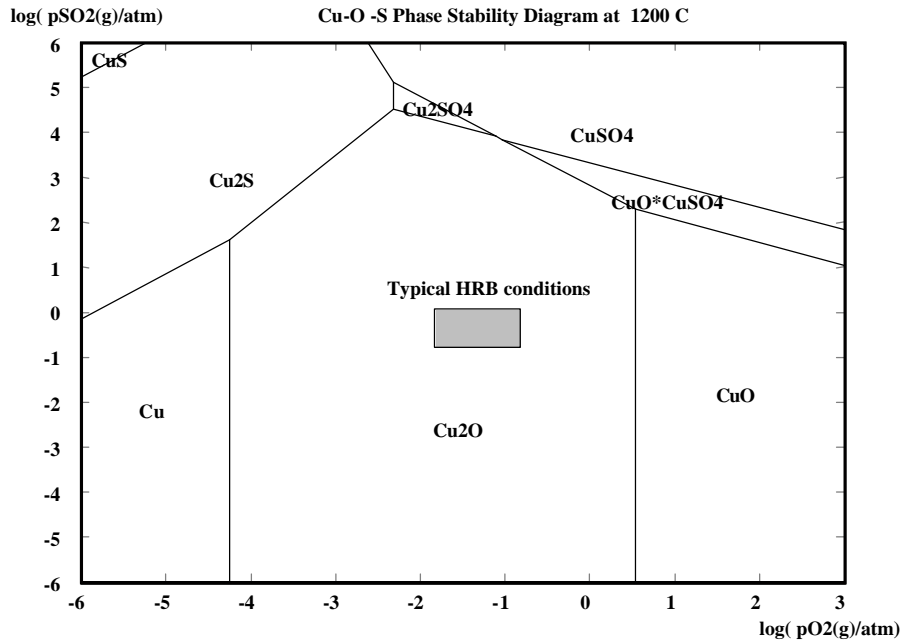
Figure 12. Phase stability diagram for Cu-O-S –system at 1200°C calculated using the HSC programme, the grey box marks typical conditions in the copper smelting heat recovery boiler inlet

3.1.1 Effects of gas parameters

<u>Temperature</u>

In Figs. 13-15 sulphate formation is illustrated as a function of temperature and reaction time with 20, 40, and 60 vol-% SO_2, and 2.5, 5, and 10 vol-% O_2 concentrations in the reaction gas. In general, the amount of sulphate increases with increasing residence time and oxygen concentration, as expected.

On the basis of these experiments, the temperature for the most effective Cu_2O sulphation lies under 600°C when SO_2 concentration is low (20 vol-%) and oxygen concentration is high (Fig. 13 e-f), and shifts up to 620°C with medium/high sulphur dioxide concentration. With high sulphur dioxide and low oxygen content in the reaction gas, the optimal temperature appears to be even slightly higher, near 640°C (Fig. 15 a-b). Increasing the amount of sulphur dioxide and reducing the oxygen concentration raises the optimal sulphation temperature. Also, a high oxygen concentration expands the favourable temperature range (Fig. 13 e-f).
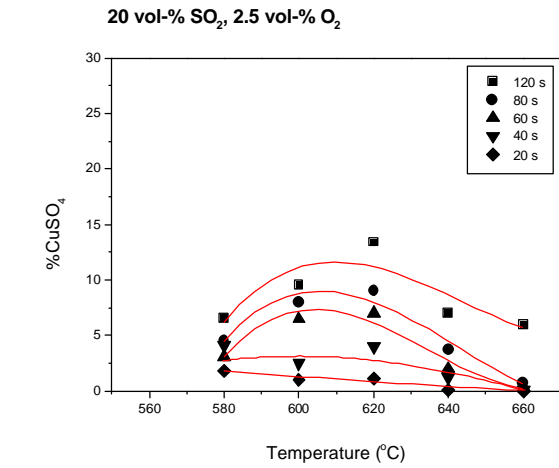
a)
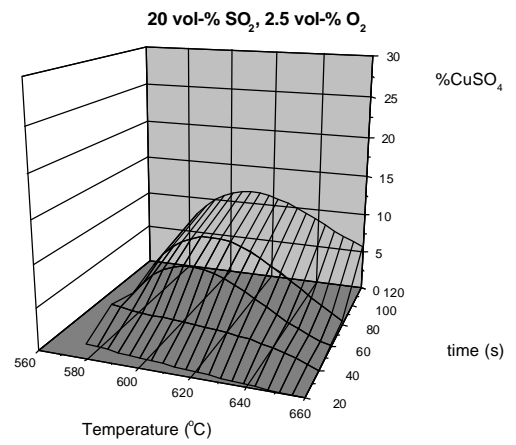
b)
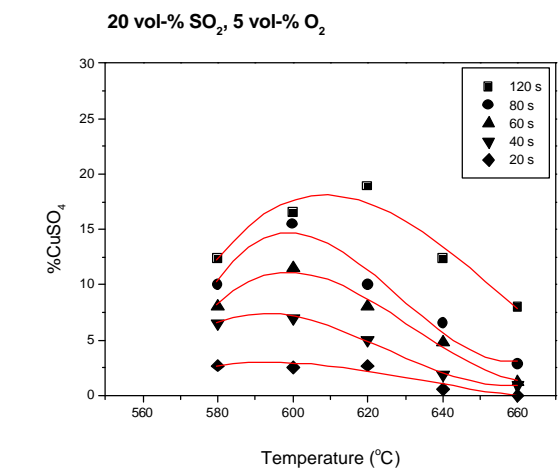
c)
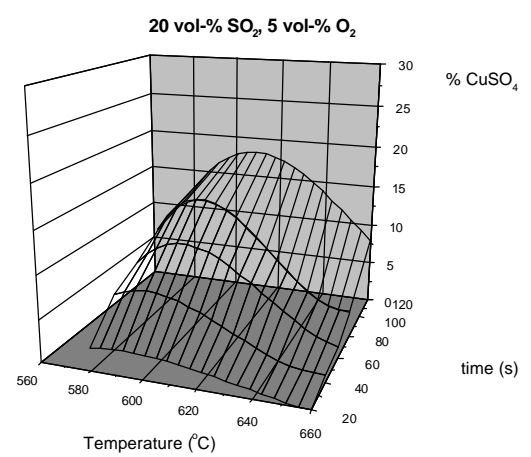
d)
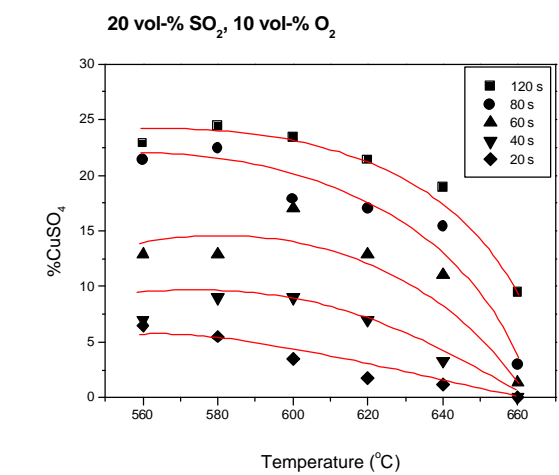
e)
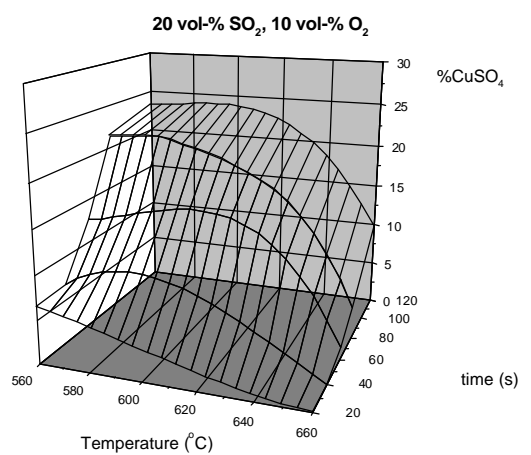
f)

Figure 13. Effects of reaction time and temperature with 20 vol-% SO₂, with a-b) 2.5 vol-% O₂, c-d) 5.0 vol-% O₂, e-f) 10.0 vol-% O₂, fraction 37–53 µm
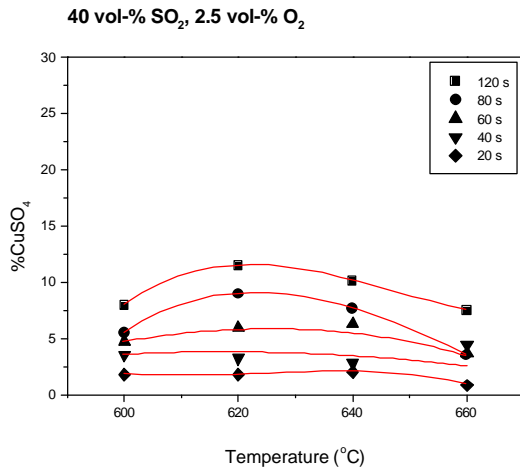
a)
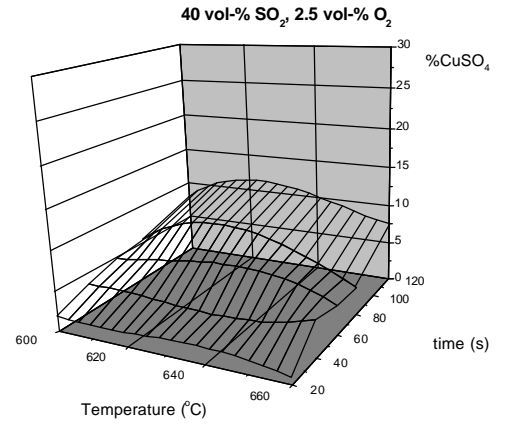
b)
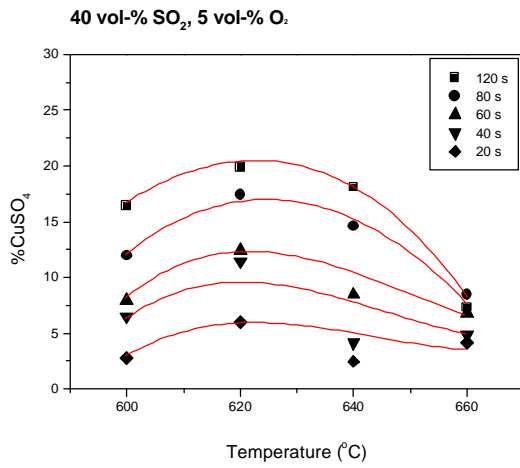
c)
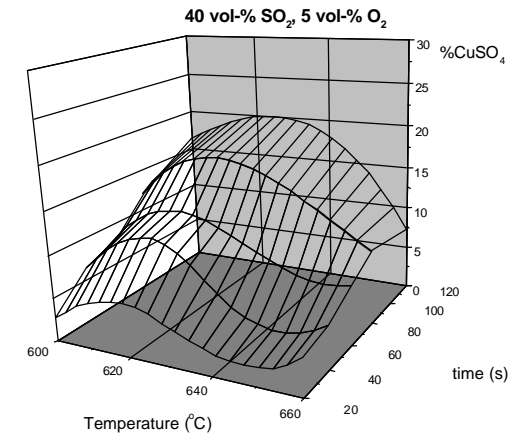
d)
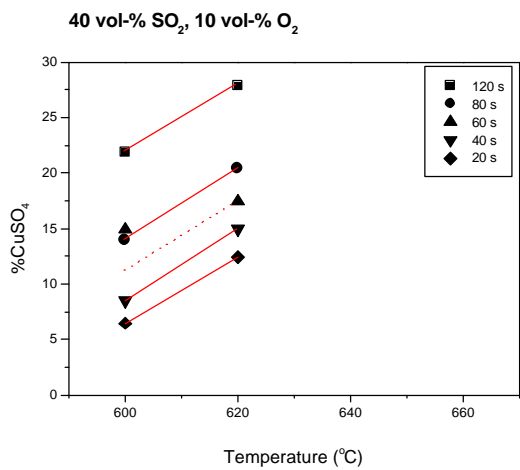
e)

Figure 14. Effects of reaction time and temperature with 40 vol-% SO₂, with a-b) 2.5 vol-% O₂, c-d) 5.0 vol-% O₂, e) 10.0 vol-% O₂, fraction 37–53 µm
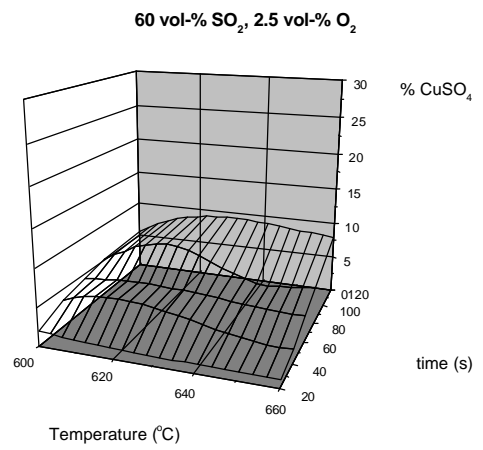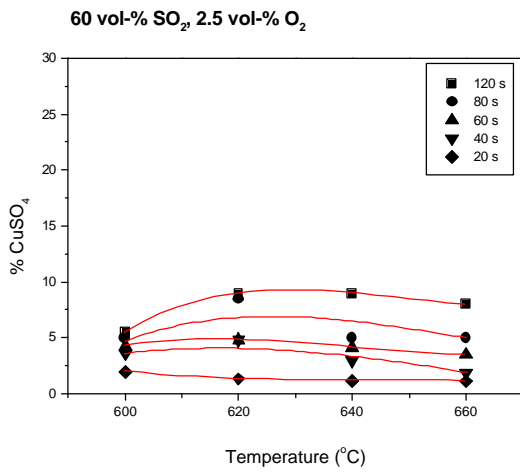
a)

b)
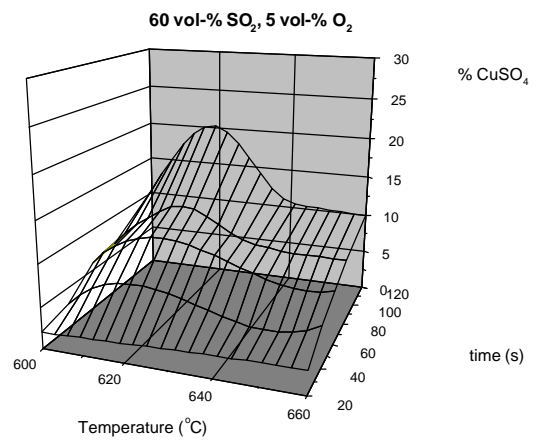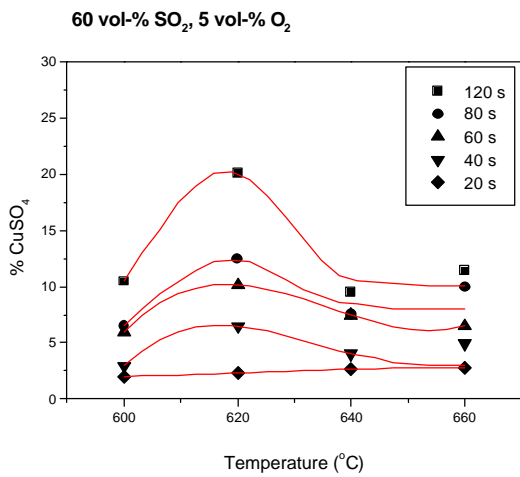
c)

d)

Figure 15. Effects of reaction time and temperature with 60 vol-% SO₂, with a-b) 2.5 vol-% O₂, c-d) 5.0 vol-% O₂, fraction 37–53 μm

Oxygen concentration

The effect of an increase in oxygen content in the reaction gas is illustrated as a function of the reaction time at 620°C in Fig. 16. Sulphate amounts increase as a function of residence time, and a slight retardation of sulphate formation is observed. Doubling the oxygen amount from 2.5 to 5 vol-% has a more significant effect than an increase from 5 to 10 vol-%. Regardless of the sulphur dioxide content, an increase in oxygen concentration enhances sulphate formation.
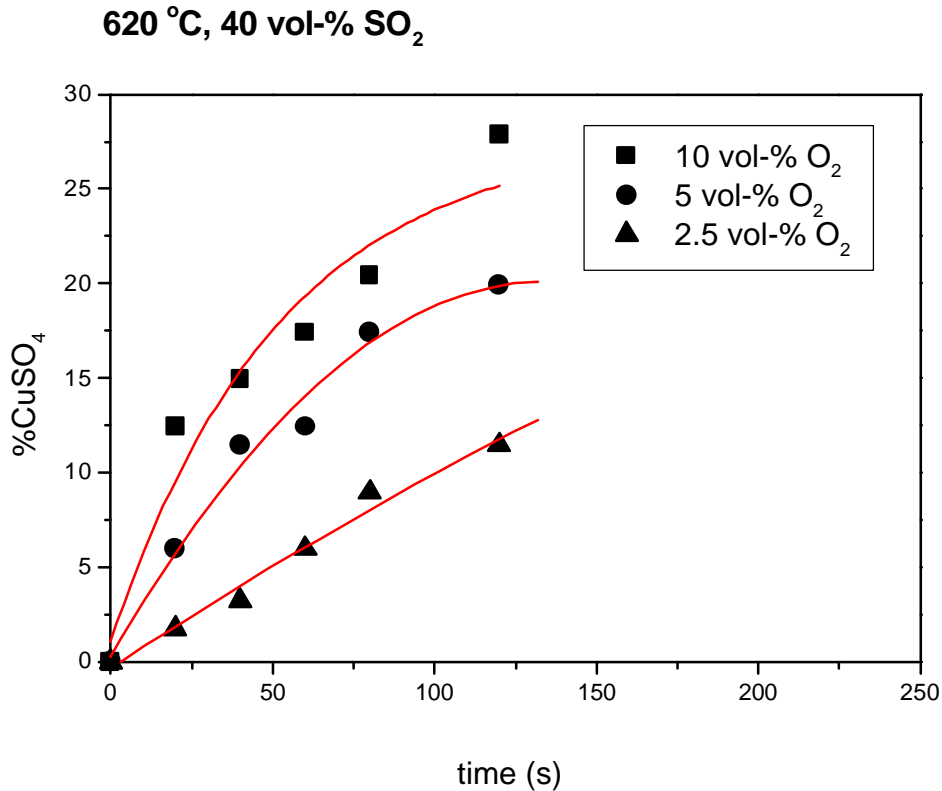
Figure 16. Results as a function of reaction time with used oxygen contents at 620°C with 40 vol-% SO$_2$, fraction 37–53 μm

Sulphur dioxide concentration

The effect of sulphur dioxide concentration (20-40-60 vol-%) with a 60-second reaction time and 5 and 2.5 vol-% oxygen concentrations is presented in Fig 17. With the lowest SO_2 concentration, the sulphation maximum is reached in the vicinity of 600°C. Higher SO_2 concentrations shift the peak closer to 620°C. A 60 vol-% SO_2 concentration leads to a lower sulphate outcome than 40 vol-%.
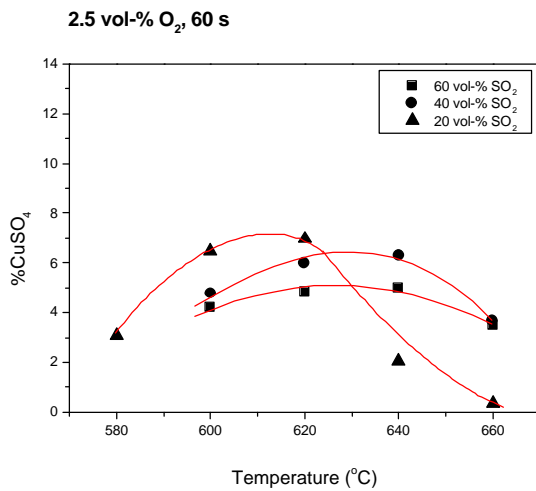
a)
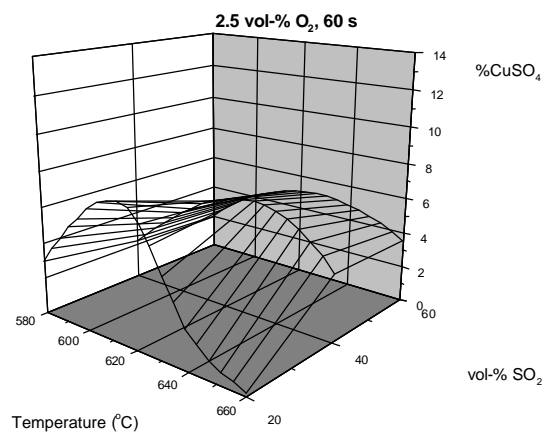
b)
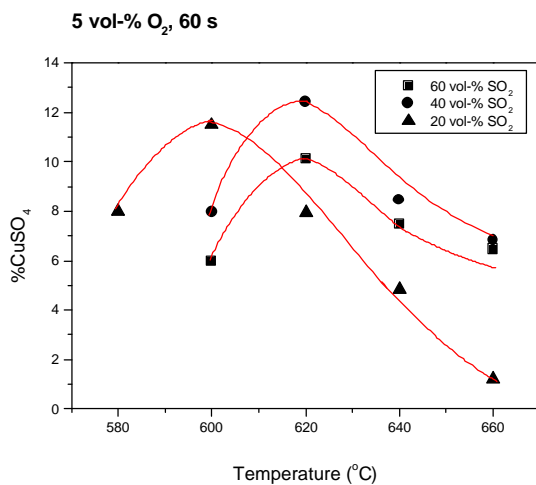
c)
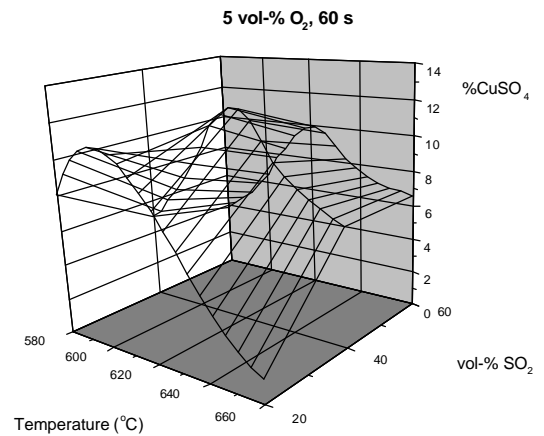
d)

Figure 17. Effects of temperature and sulphur dioxide content with 60 s reaction time with a-b) 2.5 vol-% O_2, c-d) 5.0 vol-% O_2, fraction 37–53 µm

3.1.2 Effect of particle size

The importance of the particle size is illustrated in Fig. 18. A series of experiments was conducted at 600°C with a 60-second reaction time and a gas composition of 40 vol-% SO_2 and 5 vol-% O_2. Four different screen fractions of Cu_2O were applied. As expected, the sulphation degree increases with decreasing particle size. The effect of particle size (specific surface area) is significant.
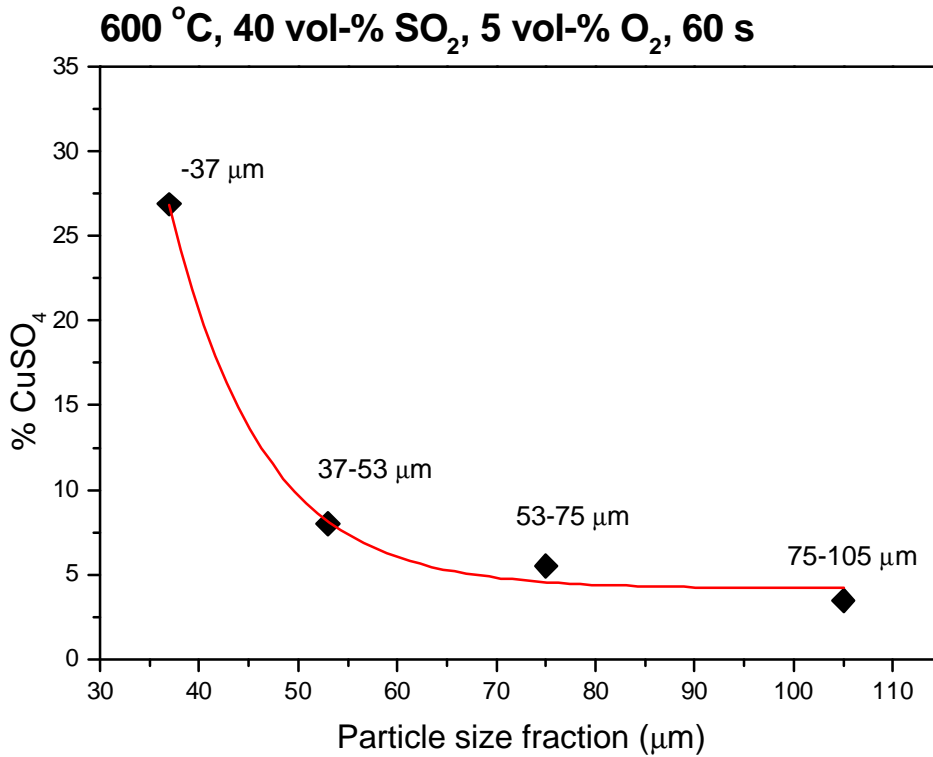
Figure 18. Effect of screen fraction on the sulphation of cuprous oxide. Experimental conditions: T = 600 °C, t = 60 s, 40 vol-% SO_2, 5 vol-% O_2.

3.1.3 Effect of Pt-catalyst

Different catalysts have a promoting effect on sulphur trioxide formation *[Kyt97, Bac86]*, which in turn is assumed to advance sulphate generation. In these experiments, platinum was used as a catalyst. A twisted platinum wire was placed at the top of the gas heating zone. The total weight of the wires was approximately 4 grams, with a diameter of 0.25 mm, giving a total surface area of 30 cm^2. The temperature in the region of the Pt wire was 30°C below the experimental temperature. The temperatures used in the current experiments (600–640°C) yield a temperature range of approximately 550–610°C in the catalyst area.

The results with and without a catalyst as a function of temperature are shown in Fig. 19. The oxygen concentration was 5 vol-%, that of sulphur dioxide 40 vol-%, and the reaction time one minute. On the basis of the experiments, sulphate formation is slightly enhanced with the use of a catalyst, but the optimal temperature moves down from the vicinity of 620 to closer to 600°C.

40 vol-% SO$_2$, 5 vol-% O$_2$, 60 s
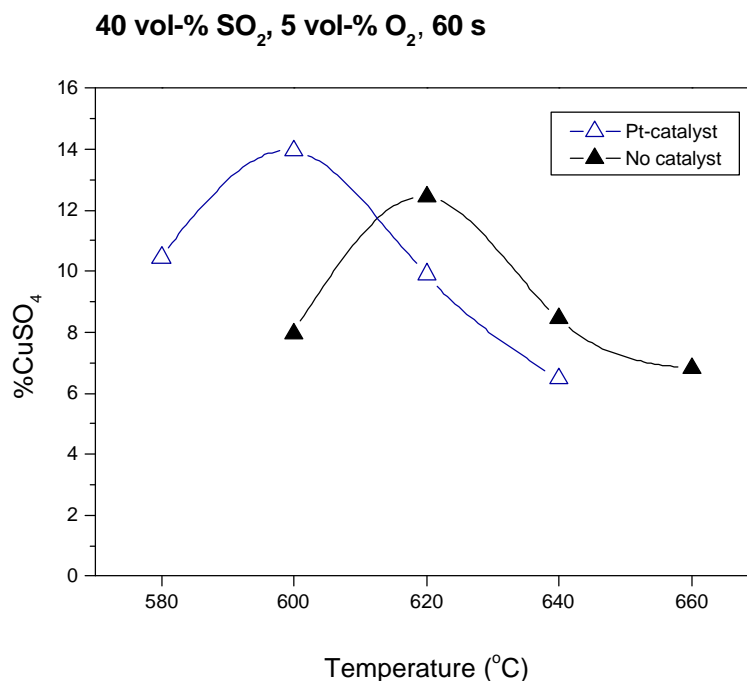
Figure 19. Effect of platinum catalyst on sulphate formation,Cu$_2$O fraction 37–53 μm

3.1.4 Microscopic examinations

<u>Surface morphology</u>

A considerable portion of the samples was examined with the SEM. As the reactions proceed, the angular shapes of the original particles disappear under the thickening product layer. The particles become more rounded and surface structures more detailed. The effects of temperature and oxygen concentration are illustrated in Fig. 20. The lower the temperature, the more detailed the typical surface pattern is.
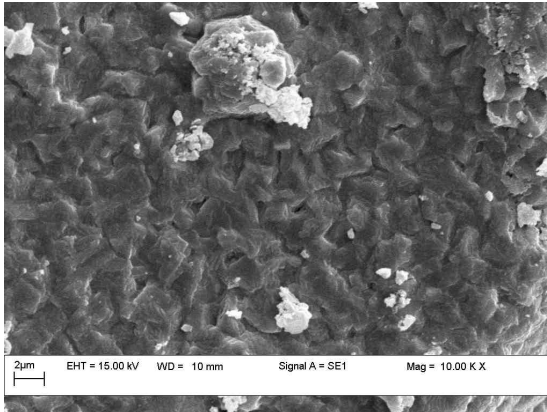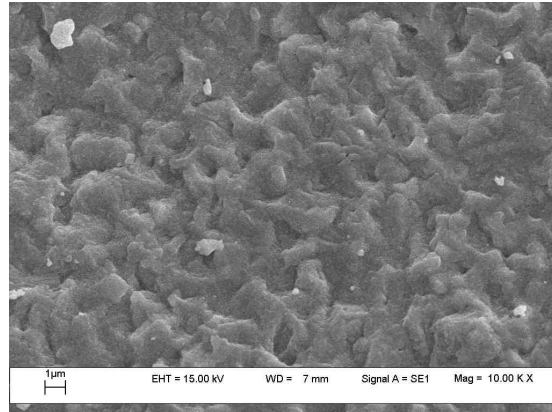
a) 600°C, 2.5 vol-% O_2

b) 600°C, 5 vol-% O_2
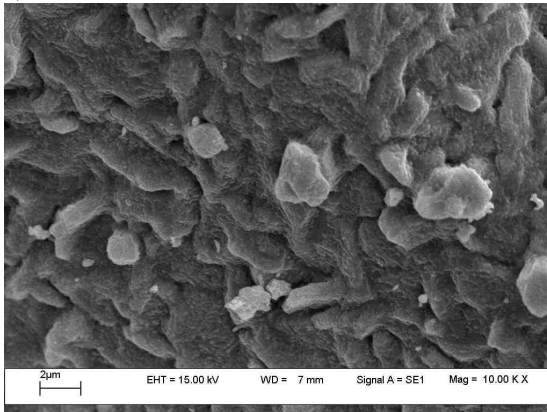
c) 620°C, 2.5 vol-% O_2
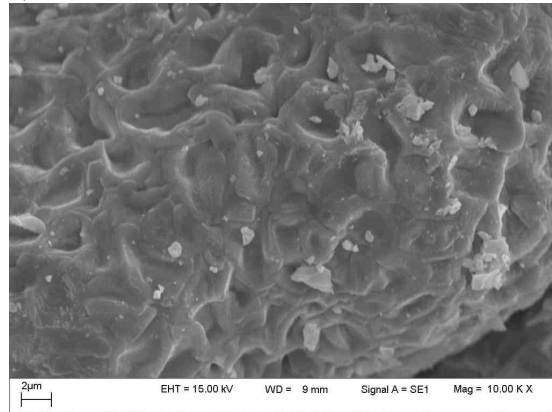
d) 620°C, 5 vol-% O_2
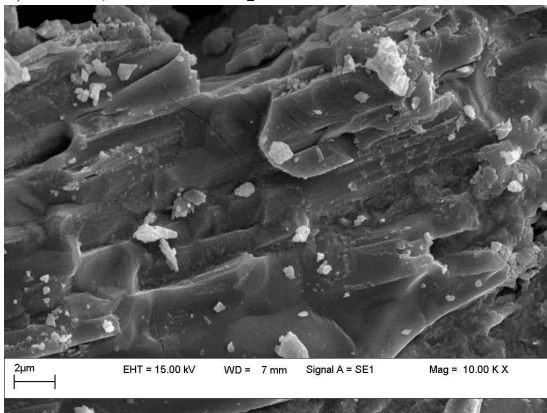
e) 640°C, 2.5 vol-% O_2
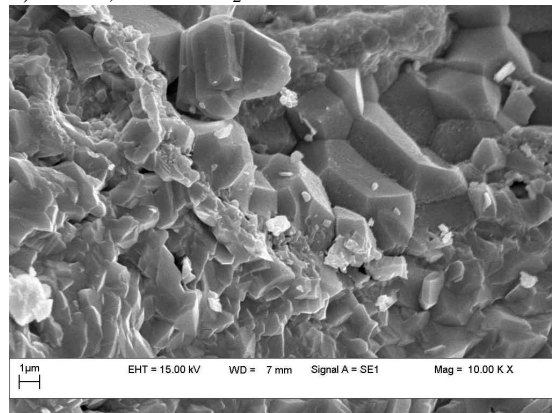
f) 640°C, 5 vol-% O_2
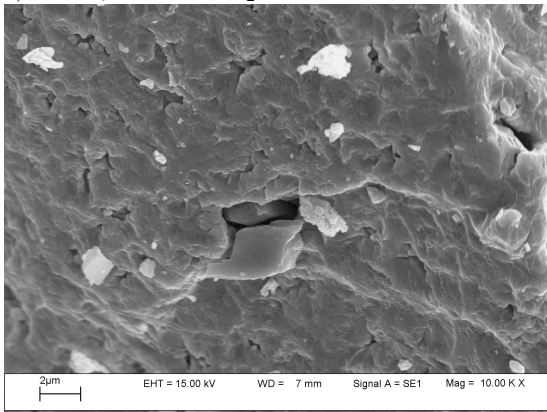
g) 660 °C, 2.5 vol-% O_2
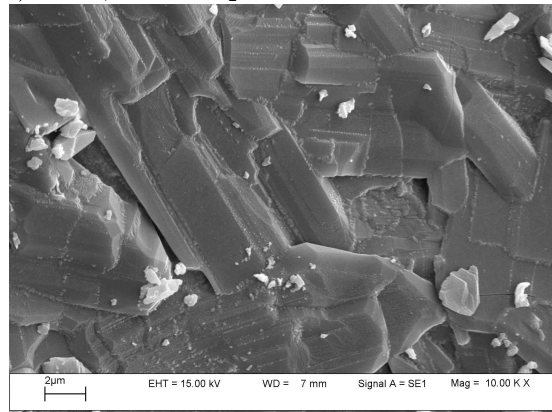
h) 660 °C, 5 vol-% O_2

Figure 20. Typical surfaces at the studied temperatures, t = 120 s, 40 vol-% SO_2, on the left 2.5 vol-% O_2, right 5 vol-% O_2

The growth of the sulphate layer as a function of the reaction time is illustrated in Fig. 21. In twenty seconds sulphate formation has just started, and the original surface is still visible. Tiny dust particles on the original surfaces (Fig. 4) may act as initial starting points for the sulphate growth. After a minute the surfaces are totally covered, and in two minutes the original shapes of the particles have disappeared. Sintering of the particles becomes more prominent, particularly with high SO_2 (Fig. 21f).

a) 20 s, 640°C, 40 vol-% SO_2, 2.5 vol-% O_2

b) 20 s, 620°C, 60 vol-% SO_2, 5 vol-% O_2

c) 60 s, 640°C, 40 vol-% SO_2, 2.5 vol-% O_2

d) 60 s, 620°C, 60 vol-% SO_2, 5 vol-% O_2

e) 120 s, 640°C, 40 vol-% SO_2, 2.5 vol-% O_2

f) 120 s, 620°C, 60 vol-% SO_2, 5 vol-% O_2
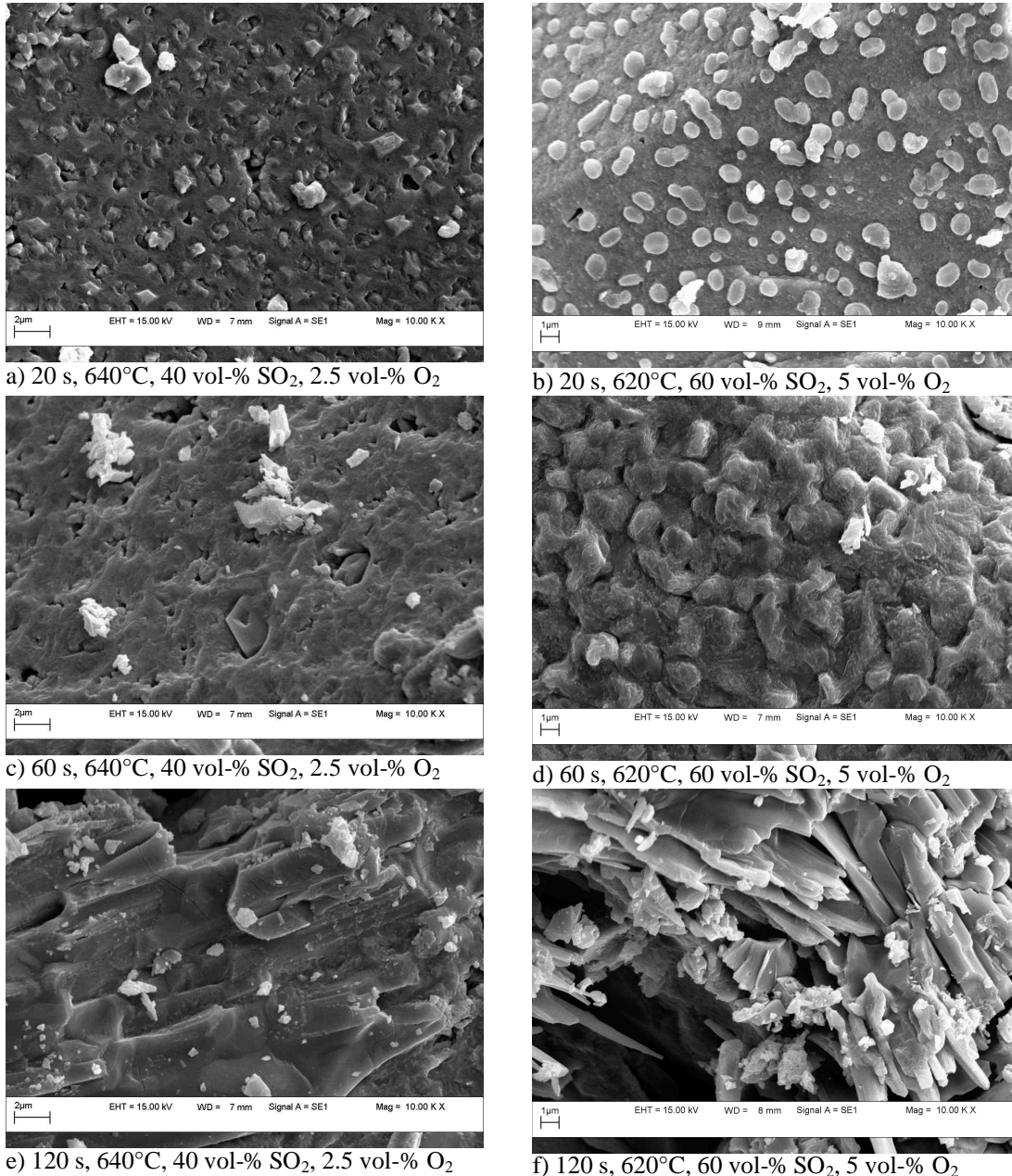
Figure 21. Changing morphology as a function of reaction time; on the left 640°C, 40 vol-% SO_2, 2.5 vol-% O_2, on the right 620°C, 60 vol-% SO_2, 5 vol-% O_2

Cross-sections

Preparing cross-sections proved to be laborious. A hard Cu_2O core surrounded by a brittle, water-soluble sulphate phase is a difficult combination to grind and polish. Quick grinding with minimal pressure using SiC-paper with ethanol as lubricant

provided the best result. Polishing was omitted totally because it flushed out most of the sulphate phase. Cross-sections were made of only selected series of samples.

Element mapping was carried out for selected samples to see the distribution of the elements. Typical result is presented in Fig. 22. Cu_2O has reacted at 620 °C for 120 seconds with 40 vol-% SO_2 and 5 vol-% O_2. Oxide core is covered by a thick, approximately 5-8 µm, sulphate layer. This sample has reached a sulphation degree of 20 wt-%. Between the sulphate cover and oxide core is a faintly detectable, thin (1 µm) sulphur-free intermediate layer. Based on EDS-analysis it is CuO.

Another illustrative cross section micrograph of the same sample is presented in Fig. 23. Sulphate layers are well attached to the oxide cores and look dense. Some sintering is noticed like in most of the samples. Particles stick together after sulphate formation has started, because sulphate layers are covering the whole particles, and there are no oxide-oxide contacts. In general, sintering advances with reaction time, and is more significant with a high sulphur dioxide compared to lower concentrations (Fig. 24).

Cu_2O Cu map

O map   S map
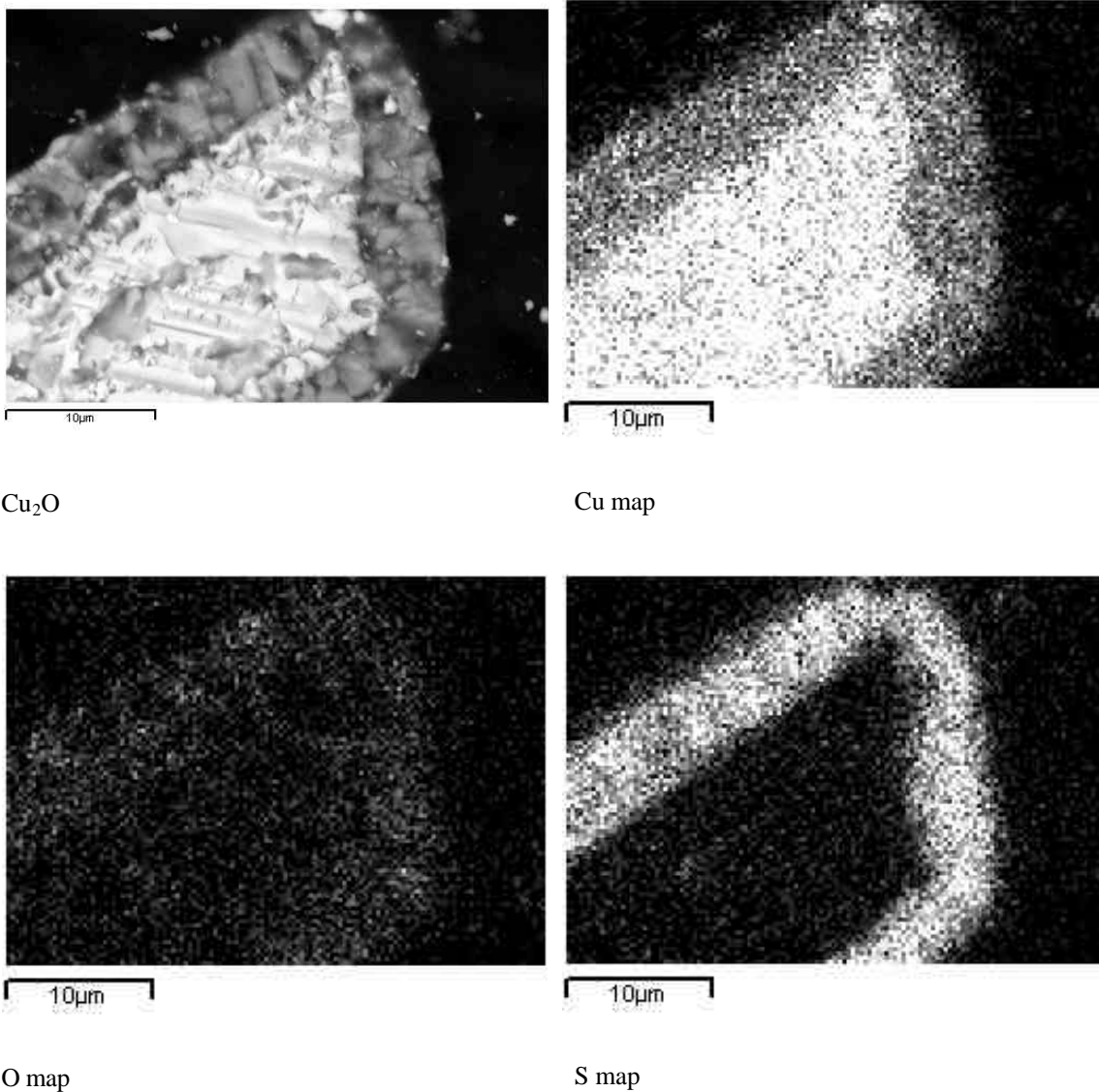
Figure 22. Element maps for a typical particle, 40 vol-% SO_2, 5 vol-% O_2, 620°C, 120 s.
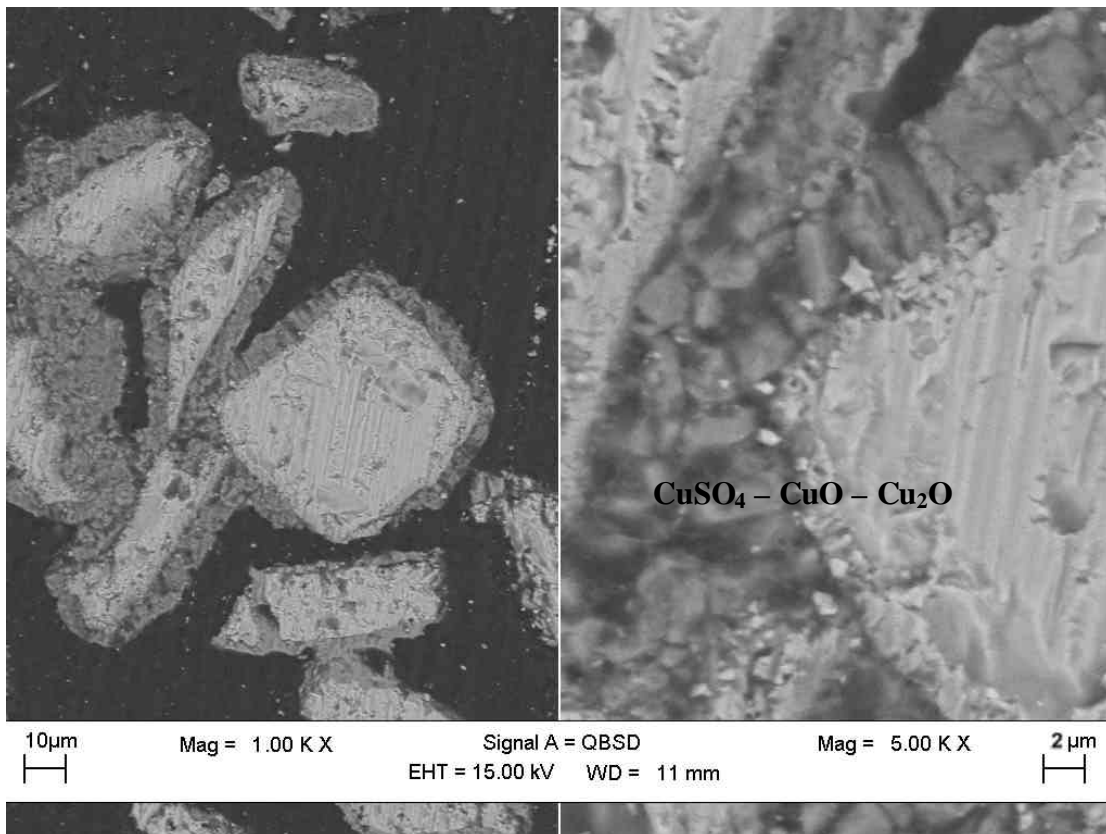
Figure 23. Group of sintered particles and closer view of the product layers. Experimental conditions: 40 vol-% SO₂, 5 vol-% O₂, 620°C, 120 s.
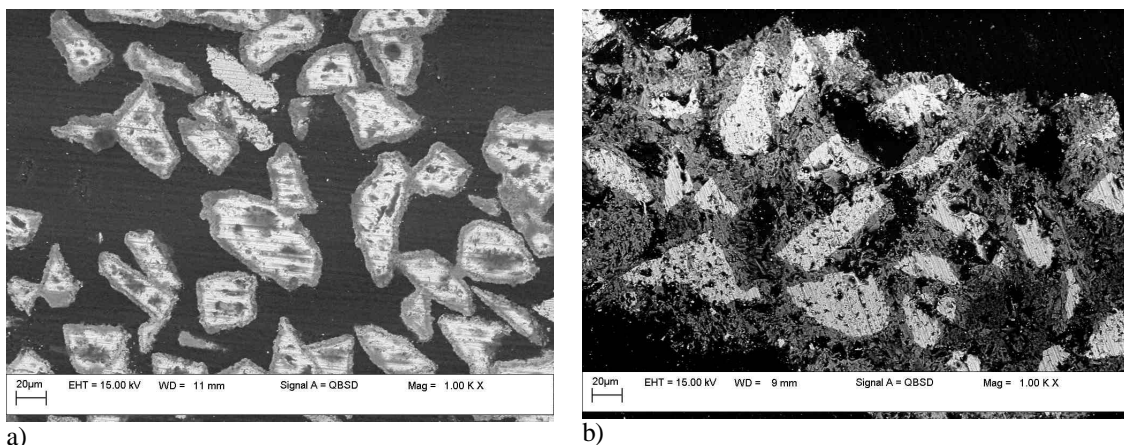
a) b)

Figure 24. Examples of sintering behaviour, effect of a) 20 vol-% SO₂ versus b) 60 vol-% SO₂ with 5 vol-% O₂, 120 s, 620 °C

Generally, particles that reacted only for a short time and/or at non-optimal sulphate formation temperature are covered by thin sulphate layers of 0-2 µm. Samples that reacted over 60 s in an atmosphere richer in oxygen (5-10 vol-%) at a favourable temperature are covered by thicker product layers. The mid-layer was found only from samples with a high degree of conversion; from others it was either missing or too thin to be detected.

In order to study the intermediate phase more closely, the sulphate layer was rinsed away from the sample in Figs. 22-23 with water using ultrasound. No sulphur was detected on the washed surface (Fig. 25b) with EDS. The revealed CuO seems clearly more porous and detailed compared to the starting Cu_2O surface (Fig 25a).
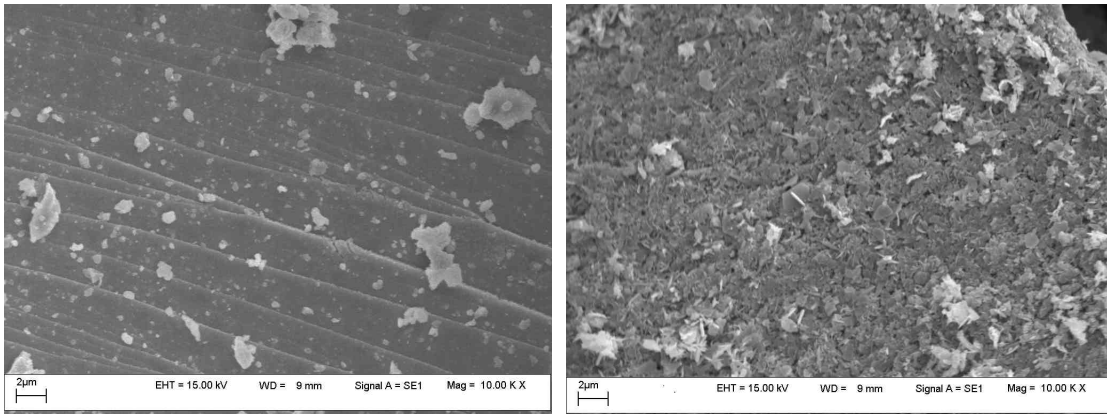
a)   b)

Figure 25.Comparison of a) original Cu₂O surface, and b) surface of a reacted sample revealed after washing (CuO)

3.1.5 Sub-micron-sized Cu$_2$O

Very fine powder was also used to find out if the sulphation behaviour is qualitatively identical with coarser fractions. However, sub-micron-sized powder tended to agglomerate heavily, and fluidisation in the reactor unit was poor. The reacted samples were clearly non-homogeneous. On the basis of visual observations, the cover of the sample cake was mostly well reacted, but in the core there remained pure red oxide. With non-homogeneous samples unsuccessful sampling action may distort the results. With short reaction times the results are consistent, but with long residence times partly scattered. The effects of temperature and reaction time are illustrated in Fig. 26. Most generous sulphate formation is attained near 600°C, as with the coarser oxide (Fig. 13c-d).

20 vol-% SO$_2$, 5 vol-% O$_2$
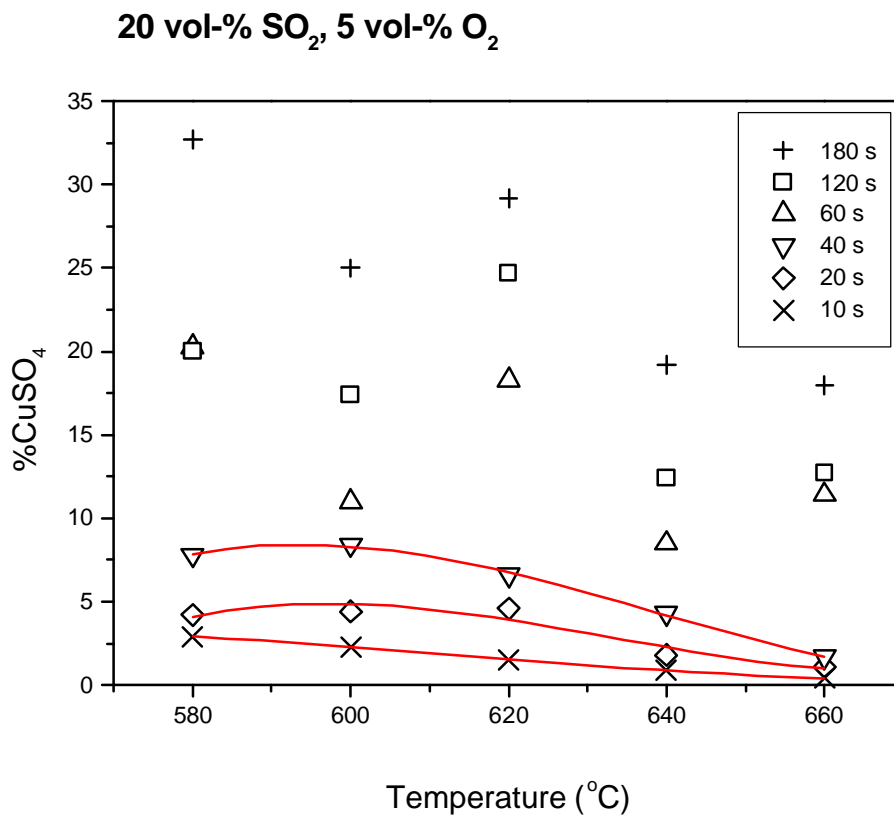
Figure 26. Effect of reaction time and temperature on the sulphation of sub-micron-sized Cu$_2$O

Compared to the coarser fraction (Fig. 27), more sulphate was formed from sub-micron feed. The effects of temperature and reaction time are similar, indicating that the different conversion results from the different specific surface areas.
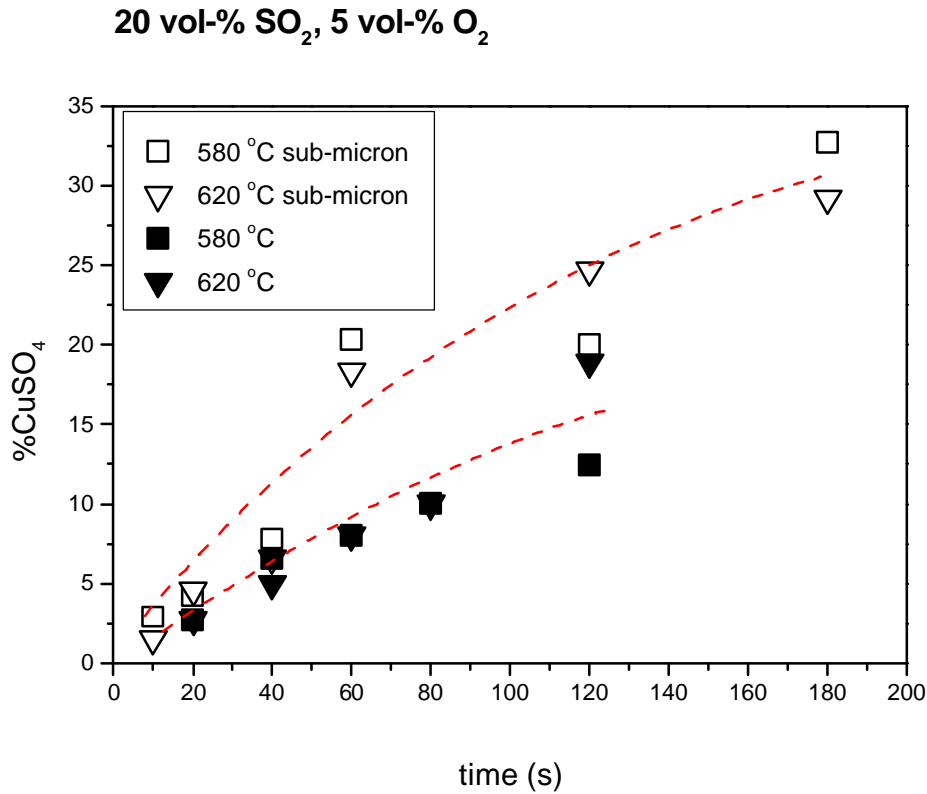
20 vol-% SO$_2$, 5 vol-% O$_2$

Figure 27. Comparison of the sulphate formation from 37-53 µm Cu$_2$O and sub-micron Cu$_2$O, 20 vol-% SO$_2$, 5 vol-% O$_2$.

To figure out if the different conversion degrees result only from the different surface areas, the reaction rates per unit surface area of sub micron sized and 37-53 µm Cu$_2$O are compared in Table I (Compare with Fig. 27). Sulphation rate per unit surface area appears to be slightly higher for the coarser cuprous oxide fraction. Due to a heavy agglomeration, the actual free surface area of the sub micron sized cuprous oxide may have been lower than what was measured. In general, the order of magnitude is the same.

Table I Reaction rates per unit surface area of sub micron sized and 37-53 µm Cu$_2$O. Used specific surface areas: Cu$_2$O 37-53 µm 0.3 m^2/g, sub micron sized 0.98 m^2/g

	CuSO4 (%) / [t (s) * A (m2/g)]			
	37-53	37-53	sub micron	sub micron
t (s)	Cu2O/ 600 C	Cu2O/ 620 C	Cu2O/ 600 C	Cu2O/ 620 C
10			0.23	0.15
20	0.41	0.46	0.23	0.23
40	0.58	0.41	0.21	0.17
60	0.64	0.44	0.19	0.31
80	0.64	0.41		
120	0.46	0.53	0.15	0.21
180			0.14	0.16

3.2 Sulphation of synthetic CuO

As the temperature decreases in the heat recovery boiler, CuO becomes the stable copper oxide phase, as shown in Fig. 28.
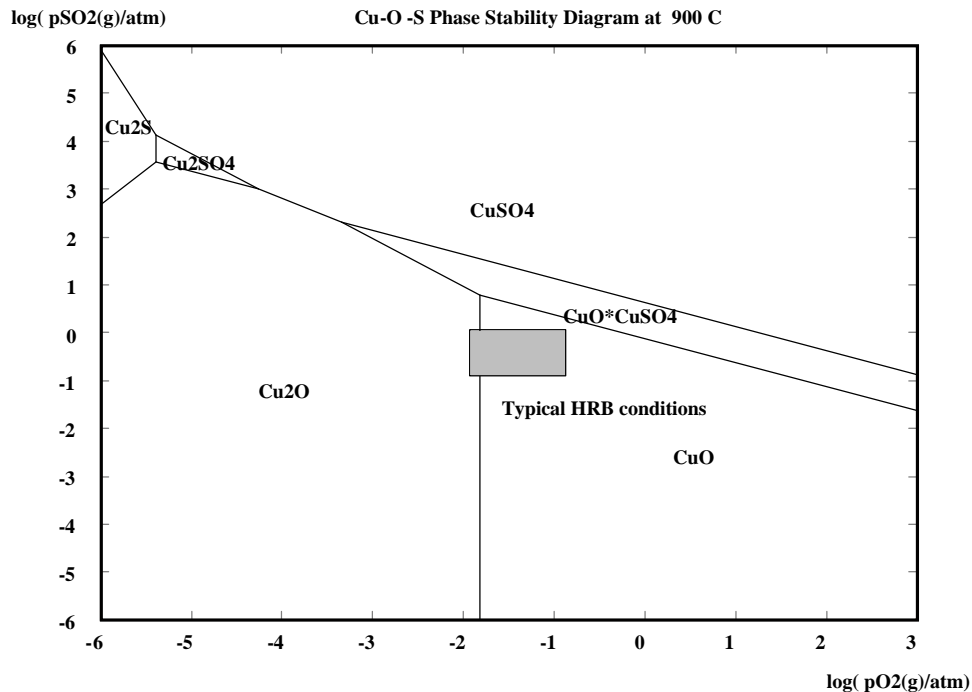
Figure 28. Phase stability diagram for Cu-O-S –system at 900°C calculated using the HSC programme, the grey box marks typical conditions in the copper smelting heat recovery boiler radiation section.

3.2.1 Effects of gas parameters

Temperature

In Fig. 29 sulphate formation is illustrated as a function of temperature and reaction time with 40 vol-% SO_2 and 2.5 and 5 vol-% O_2 concentrations of the reaction gas. In general, the effect of temperature is not as significant as it is with Cu_2O in the studied temperature range. On the basis of these experiments, the temperature for maximum CuO sulphation lies in the vicinity of 620°C when the oxygen concentration is 5.0 vol-% and shifts closer to 640°C with a lower oxygen concentrations.
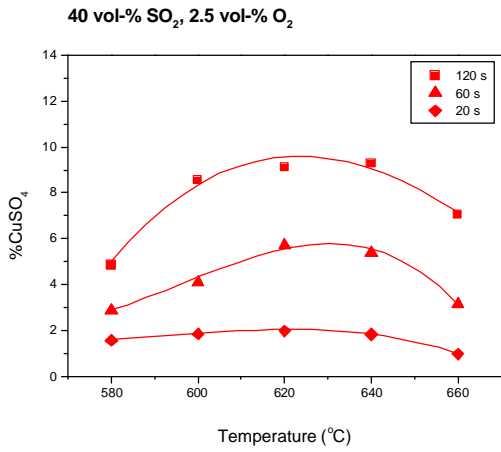
a)
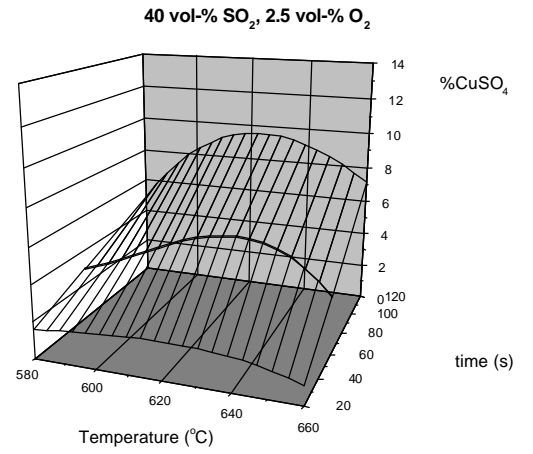
b)
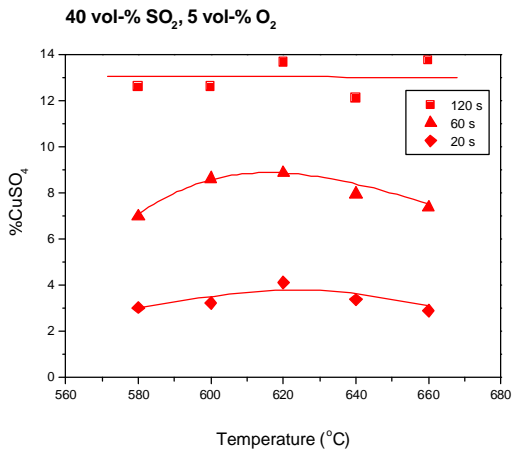
c)
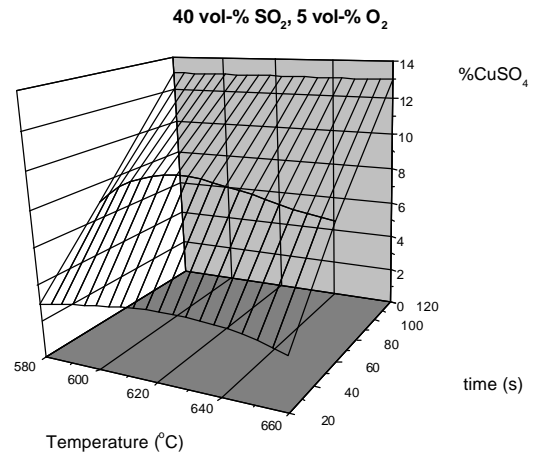
d)

Figure 29. Effects of reaction time and temperature with 40 vol-% SO₂, with a-b) 2.5 vol-% O₂, c-d) 5.0 vol-% O₂

Oxygen concentration

Sulphate amounts increase as a function of residence time, and retardation of sulphation rate is not very substantial even in extended residence times (Fig. 30). An increase in oxygen content significantly enhances sulphation.

40 vol-% SO$_2$, 620 ^{o}C
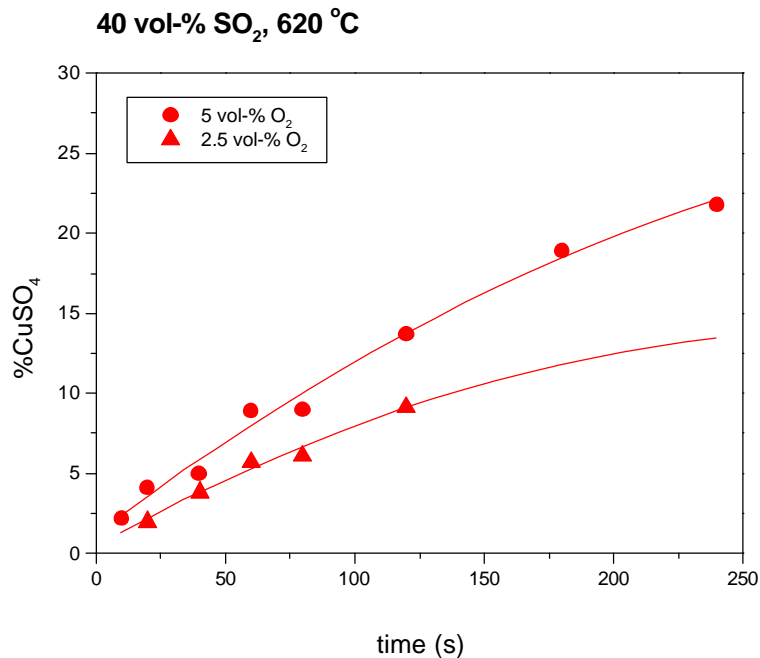
Figure 30. Effect of residence time and oxygen concentration on the sulphation of CuO

Sulphur dioxide concentration

The effect of sulphur dioxide concentration is illustrated in Fig. 31. 40 vol-% sulphur dioxide leads to a higher sulphate outcome compared to 20 vol-%.

5 vol-% O$_2$, 60 s
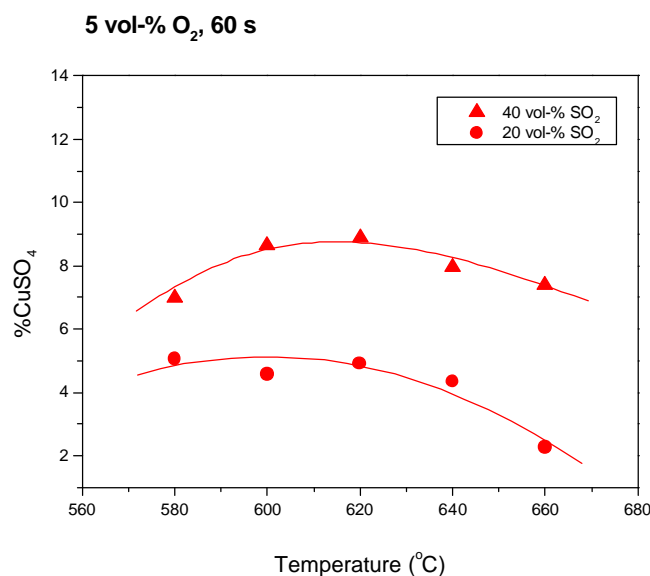
Figure 31. Effect of sulphur dioxide concentration (20 vol-% versus 40 vol-%) on the sulphation of CuO

3.2.2 Microscopic examinations

<u>Surface morphology</u>

In general, the morphology of the reacted cupric oxide samples corresponds to the reacted cuprous oxide. The disappearance of the original surface shapes as a function of residence time is illustrated in Fig. 32.

a) 10 s

b) 60 s

c) 180 s

d) 240 s
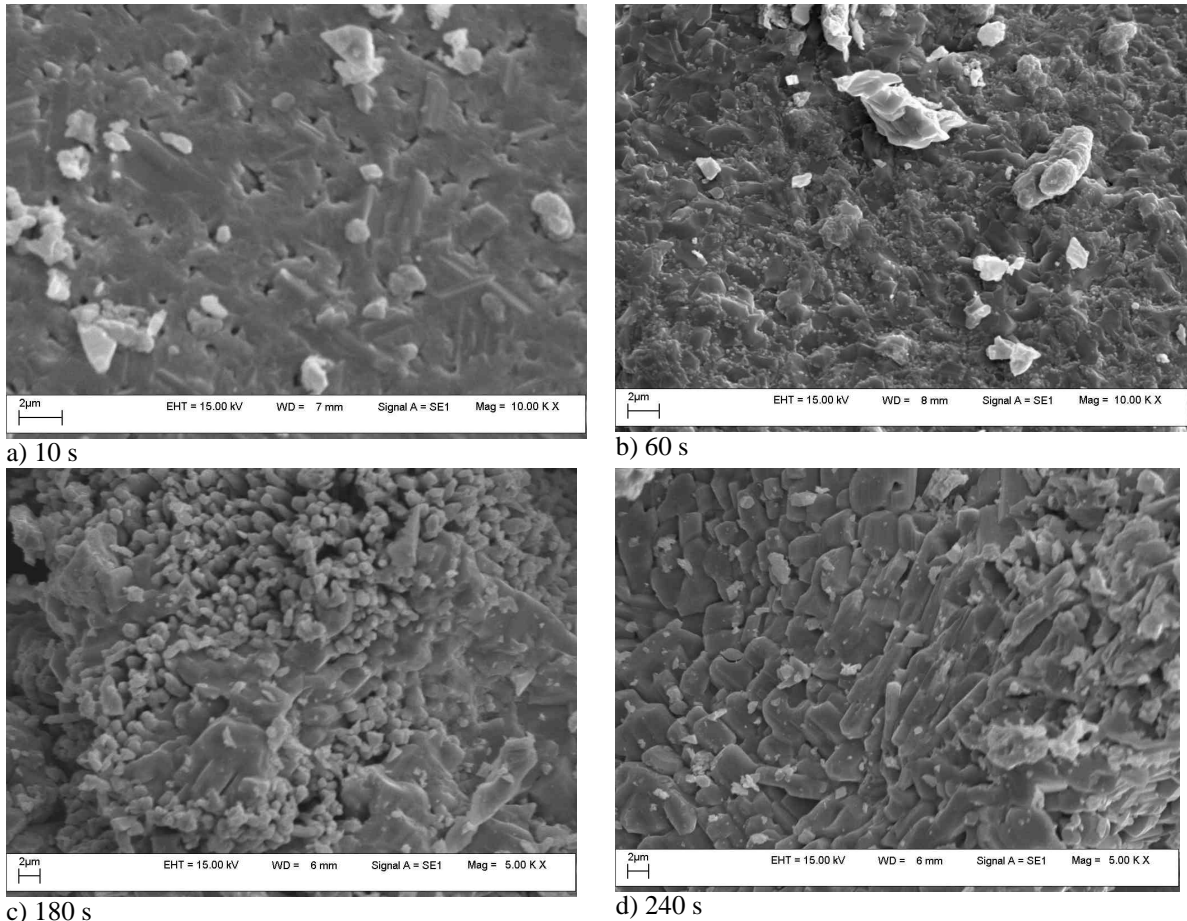
Figure 32. Changing morphology as a function of reaction time; 620°C, 40 vol-% SO_2, 5.0 vol-% O_2.

Cross-sections

Element maps of a typical sulphated CuO particle are shown in Figure 33. In the core is the oxide phase, which is surrounded by a dense sulphate shell.
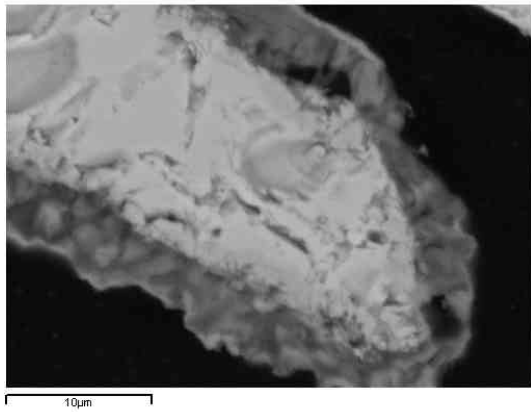
CuO
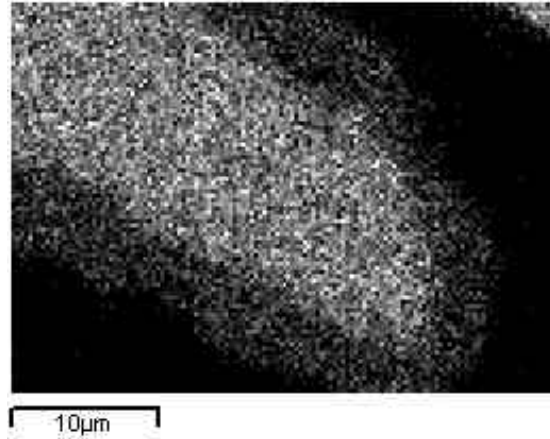
Cu map
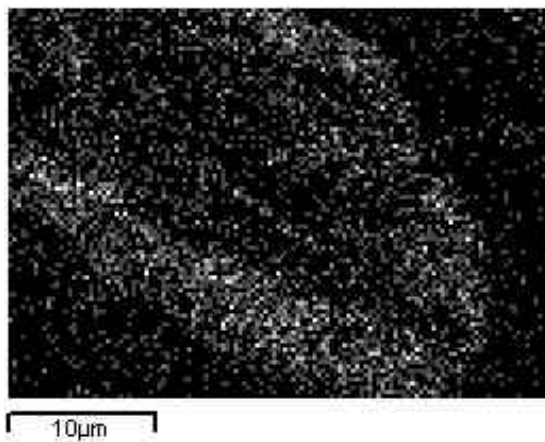
O map
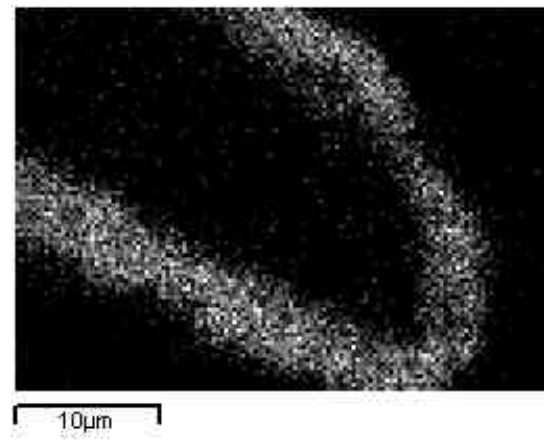
S map

Figure 33. Element maps for a reacted particle. Experimental conditions: 40 vol-% SO$_2$, 5 vol-% O$_2$, 620°C, 120 s.

The sulphate layer becomes thicker along with the residence time. After twenty seconds the product layer is approximately 1 µm, and post two minutes roughly 3-4 µm (Fig. 34).

a)   b)
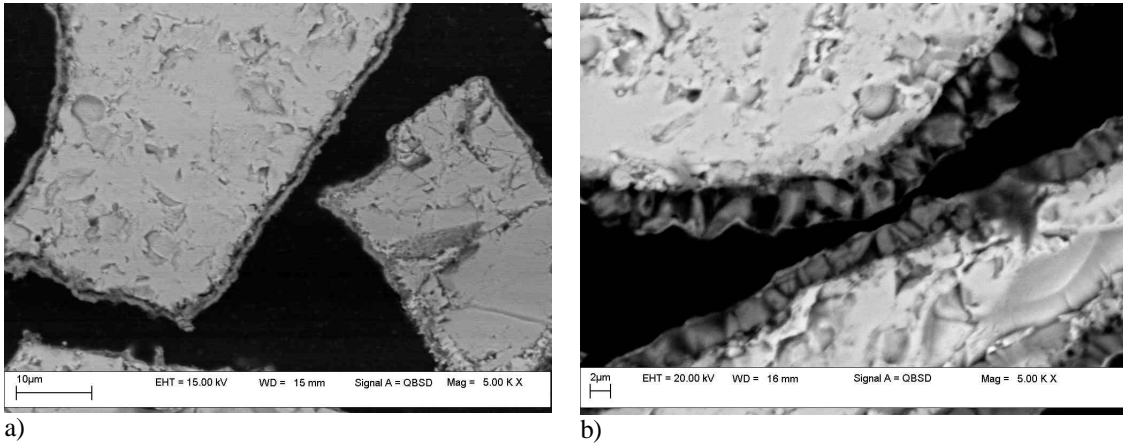
Figure 34. Thickness of the product layer in a) 20 s b) 120 s, Experimental conditions: 40 vol-% SO$_2$, 5 vol-% O$_2$, 620°C.

The outer sulphate surface is similar to that of the sulphated cuprous oxide. To see the CuO surface beneath, the sulphate phase was rinsed off from a selected sample. The exposed CuO surface (Fig. 35) is now more detailed compared to the initial oxide, but is clearly less porous than the washed Cu$_2$O (Fig. 25b).
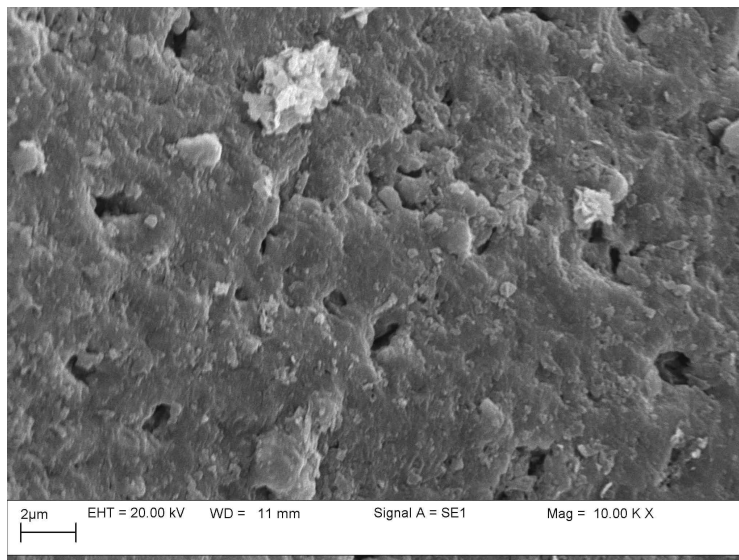
Figure 35. Sulphur-free CuO surface exposed after washing, experimental conditions: 40 vol-% SO$_2$, 5 vol-% O$_2$, 620°C, 120 s.

3.3 Sulphation of partially oxidised Cu matte

Of the materials tested, the partially oxidised matte best corresponds to the process dust, both as regards size and chemical composition. *[Sam01a-b]*

3.3.1 Effects of temperature and reaction time

Right at the beginning, sulphate formation is very intensive, in the whole tested temperature range, and slows down with time (Fig. 36). The lowest tested temperature (560°C) yields the highest sulphate formation, and the highest temperature (640°C) results in the lowest outcome. The temperature dependency is illustrated in Fig. 37. The actual optimal temperature could be even lower than what was examined.

The slight inconsistency of the results may derive from the non-homogeneous feed and small sample size.
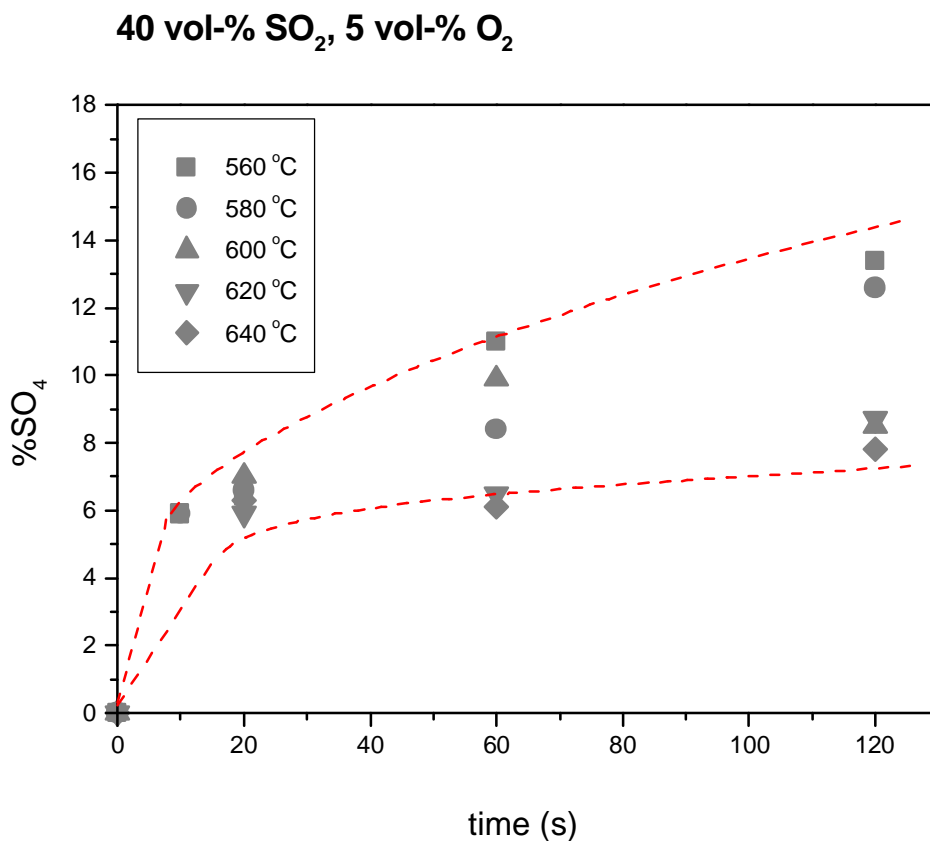
Figure 36. Effect of the reaction time on the sulphation of partially oxidised Cu matte

40 vol-% SO$_2$, 5 vol-% O$_2$
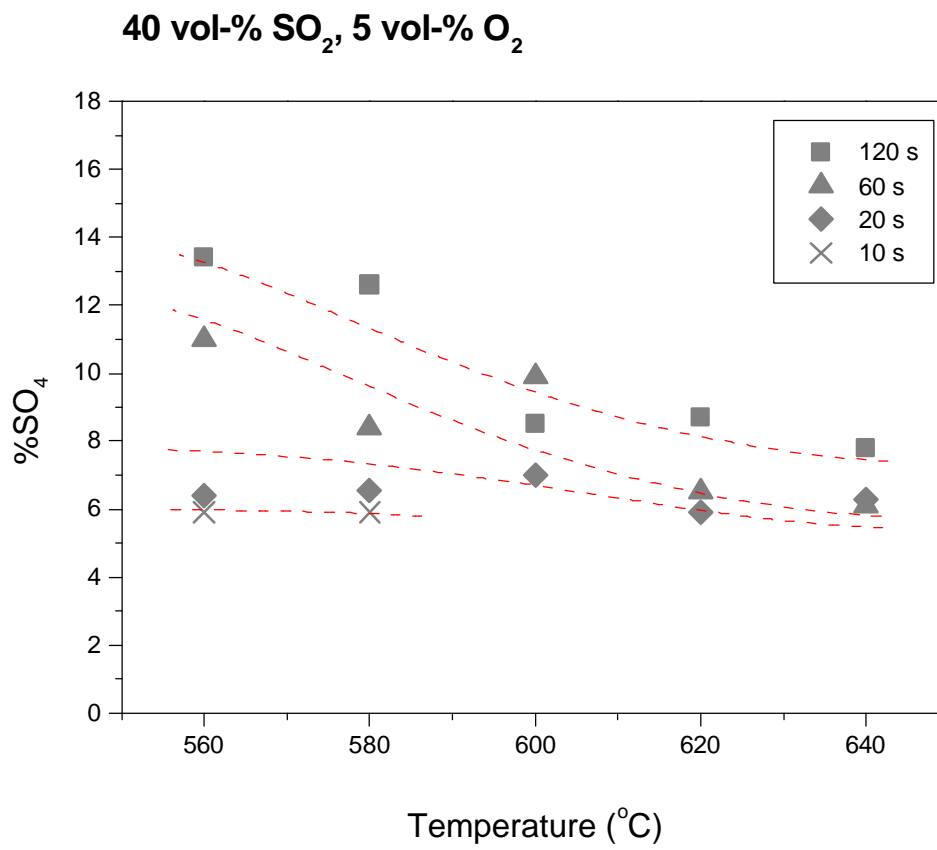
Figure 37. Effect of reaction temperature on the sulphation of partially oxidised Cu matte

3.3.2 Microscopic examinations

Morphology

Typical micrographs of small and larger particles are shown in Fig 38. The sulphate layer covers the particles, and tiny satellite particles are attached to the bigger ones. The finest particles have attained a total conversion. In general, sintering became more notable with increasing conversion.
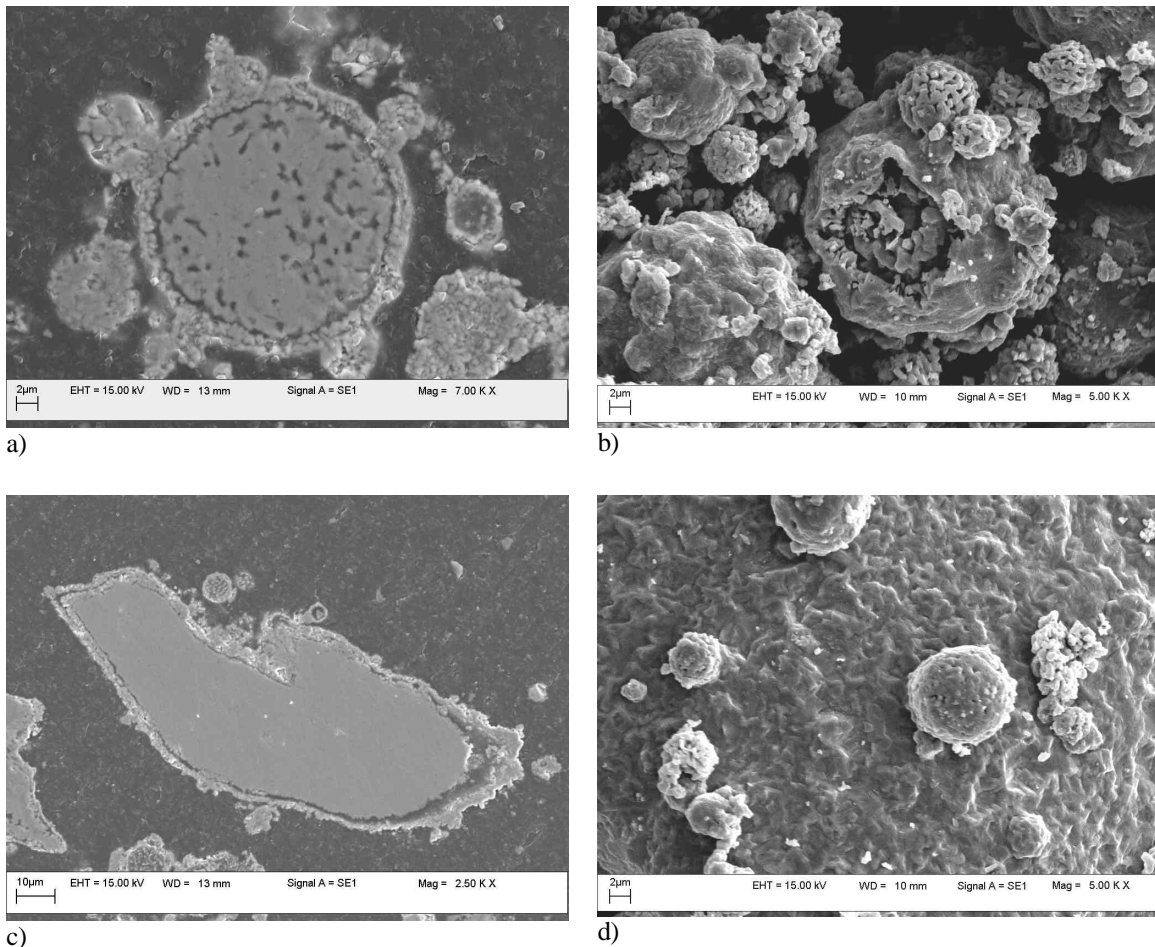
Figure 38. Cross-sections and morphology images of the sulphated matte; reaction conditions: T = 620°C, SO$_2$ 40 vol-%, O$_2$ 5 vol-%, t = 120 s. a-b) Tiny satellite particles sintered to the small main particle, c-d) large particle: copper sulphide core, Cu/Fe-sulphate cover.

3.4 Comparison of the results

The formation of sulphate from cuprous and cupric oxide as a function of temperature is compared in Fig. 39. With short reaction times and in a low oxygen partial pressure, the sulphate conversions are practically on the same level in Cu_2O and CuO. With longer residence times and favourable reaction conditions, the differences become substantial; more sulphate is formed out of cuprous oxide. Also, cuprous oxide appears to be more sensitive to temperature than cupric oxide.

a)   b)
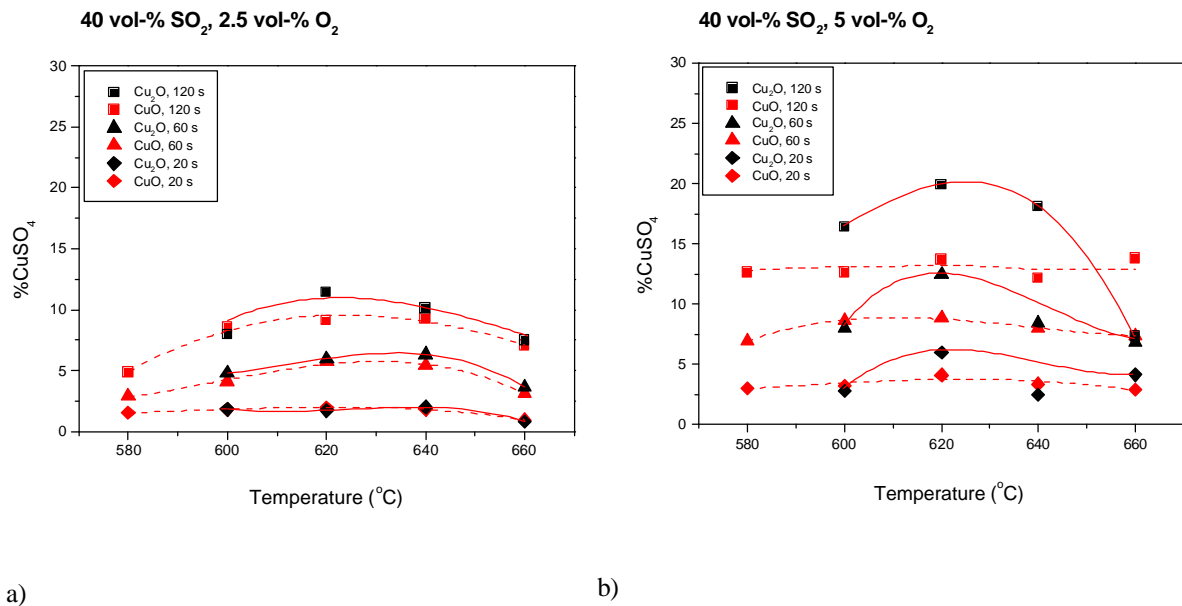
Figure 39. Comparison of the sulphation of cuprous and cupric oxide; experimental conditions: 40 vol-% SO_2, a) 2.5 vol-% O_2 b) 5.0 vol-% O_2

One phenomenon stands out clearly when comparing the synthetic and non-synthetic materials (Fig. 40): the partially oxidised matte reacts significantly faster right at the beginning. With short residence times, 10-20 s, sulphate formation is roughly fivefold in case of the partially oxidised matte compared to synthetic oxides, fraction 37-53 µm. Also the specific surface area of the partially oxidised matte is roughly fivefold compared to 37-53 µm CuO and Cu_2O.

The non-porous sub-micron-sized cuprous oxide initially reacts slowly, but exceeds oxidised matte in time, even if the experiments were carried out in lower sulphur dioxide concentration (20 vol-%) (Fig. 41).
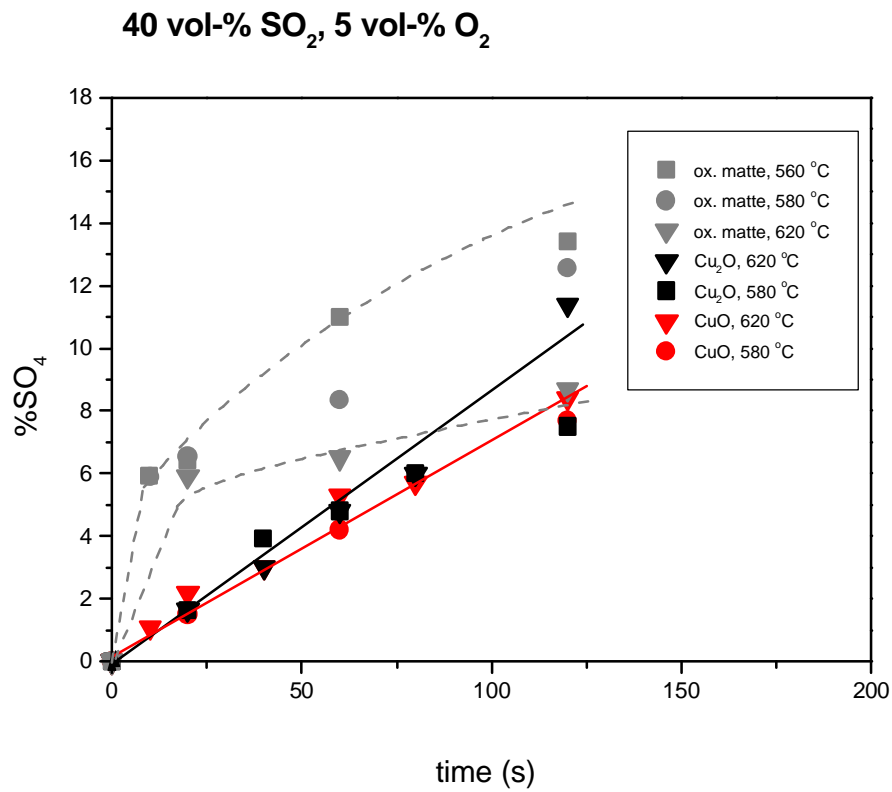
Figure 40. Comparison of the sulphation behaviour of the synthetic Cu₂O and CuO and oxidised matte.
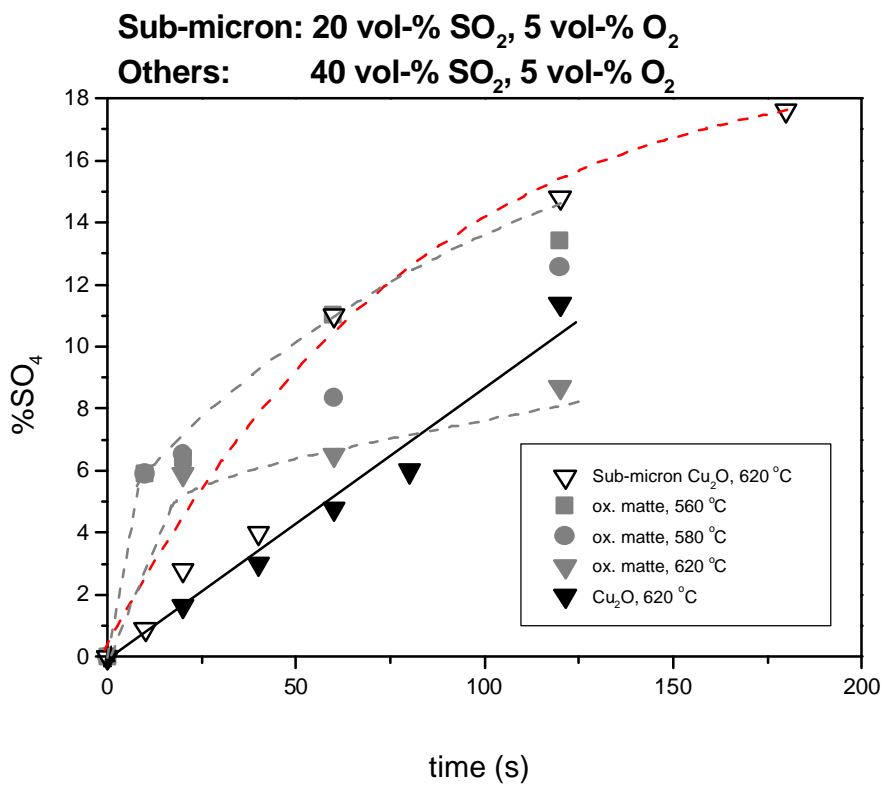
Figure 41. Comparison of the behaviour of oxidised matte, sub-micron Cu₂O, and coarse Cu₂O. Note the different SO₂ concentrations.

Reaction rates per unit surface area for CuO (37-53 µm), Cu_2O (37-53 µm) and partially oxidized matte are collected in Table II (Compare with Fig. 40). On the basis of the current results initial sulphation rate per unit surface area seems to be higher for the partially oxidised matte compared to synthetic oxides (CuO, Cu_2O).

Table II Reaction rate per unit surface area for CuO (37-53 µm), Cu_2O (37-53 µm) and partially oxidised matte. Used specific surface areas: Cu_2O and CuO 37-53 µm 0.3 m^2/g, matte 1.21 m^2/g

t (s)	SO4 (%) / [t (s) * A (m2/g)]						
	CuO/ 620 C	CuO/ 580 C	Cu2O/ 620 C	Cu2O/ 580 C	matte/ 560 C	matte/ 580 C	matte/ 620 C
10	0.37				0.49	0.49	
20	0.37	0.25	0.27	0.27	0.26	0.27	0.24
40	0.25		0.25	0.32			
60	0.29	0.23	0.27	0.27	0.15	0.12	0.09
120	0.23	0.21	0.32	0.21	0.09	0.09	0.06

4 DISCUSSION

Copper sulphate formation was found to be sensitive to gas composition and temperature. Both the particle size (specific surface area) and surface morphology have significant effects on the sulphation rate.

The results with Cu_2O as a function of particle size explain the lower conversion of synthetic cuprous oxide compared to industrial process dust. The effect of particle size (specific surface area) was noticed to be significant when the size range mostly used here, 37-53 μm, was compared with the size of typical industrial dust, -37 μm.

One phenomenon stands out clearly when comparing synthetic and non-synthetic materials: the partially oxidised matte reacts significantly faster right at the beginning. The explanation lies in both the partly smaller particle size (i.e. larger specific surface area) and more detailed surface structure. A detailed surface offers a more generous number of nucleation points for the sulphation reactions compared to flat surfaces.

In the case of oxidised matte, in addition to copper sulphate, ferric sulphate is also expected. On the basis of thermodynamic calculations, the maximum stability temperature for ferric sulphate is below 700°C at the studied conditions, while for copper sulphate it is well over 700°C *[Yan97]*. The optimal temperature for sulphate formation could be even lower than what was examined. Also, impurities (not analysed) of the feed may make some contribution to the outcome.

4.1 Conversion degree

In an industrial smelter the chemical composition and mineralogy of the flue dust depend on the type of feed concentrate and smelting practice. Matte grade varies between the smelters, and so do the oxygen and sulphur dioxide concentrations. If the oxygen content of the process gas is increased, the sulphidic phases disappear completely and the dust eventually becomes totally oxidised and sulphated. *[Sam01a-b]*

Markova *et al. [Mar00]* have investigated the compositions of flue dusts from the HRB and ESP after Outokumpu-type FSF at MDK-AD-Pirdop (Bulgaria). Samples were collected from the boiler inlet, radiation section, and convection section. The prevailing phase in all the samples was magnetite, Fe_3O_4, while the presence of hematite, Fe_2O_3, was considerably smaller. The second main phase was $CuSO_4$. Copper in sulphate form accounted for 38-45% of the total copper; in the samples from the boiler convection section the share was even slightly higher. The copper content as Cu_2O (free or connected as $Cu_2O·Fe_2O_3$) was about 30% of the total copper. The amount of copper in sulphide form (Cu_2S) decreased when moving from the boiler radiation section to the convection section, from 20 to 8-10% of the total amount of copper. Some ferrite copper ($CuFe_2O_4$) was also noticed, as well as minor amounts of $FeSO_4$.

Flue dust in the heat recovery boiler of the Outokumpu Harjavalta Cu-FSF consists mainly of particles which have a Cu-Fe-oxide core with a Cu-sulphate cover. The main component is $CuSO_4$ (approximately 40%), which binds 70-75% of the copper in dust. In second place is $CuFeO_2$, 33%. $CuFe_2O_4$ has also been identified *[Pel01]*.

The flash converting dust differs from the flash smelting dust in some degree. The most important difference is in the iron content; in the flash converting dust iron content is very low (< 3 %), in the flash smelting significantly higher (> 20 %). Also, the copper content of FC dust is higher (75 %) than that of FS dust (40 %). The non-sulphated copper in FC dust is as Cu_2O, in FS dust as $CuFeO_2$. *[Kyt97]* The studied partially oxidised Cu matte is actually closer to the flash converting dust than the flash smelting dust.

Samuelsson et al *[Sam01b]* have measured specific surface areas of two different dusts with complex mineralogy collected from copper smelter (Boliden Mineral AB), dust 1. sulphide-oxide –type, and dust 2. oxide-sulphate –type. Dusts were sieved to –36 microns, and specific surface areas of the sieved and non-sieved fraction were measured using BET-method. Dust 1. had a smaller median size and larger specific surface area than dust 2. Specific surface areas of these dusts and here studied materials are compared in Fig. 42. The process dust is smaller in size, compared to the mainly used screen fraction, 37-53 µm, and has significantly larger specific surface area. Of the tested materials, the partially oxidised matte has the largest specific surface area, and it was found to be most reactive.
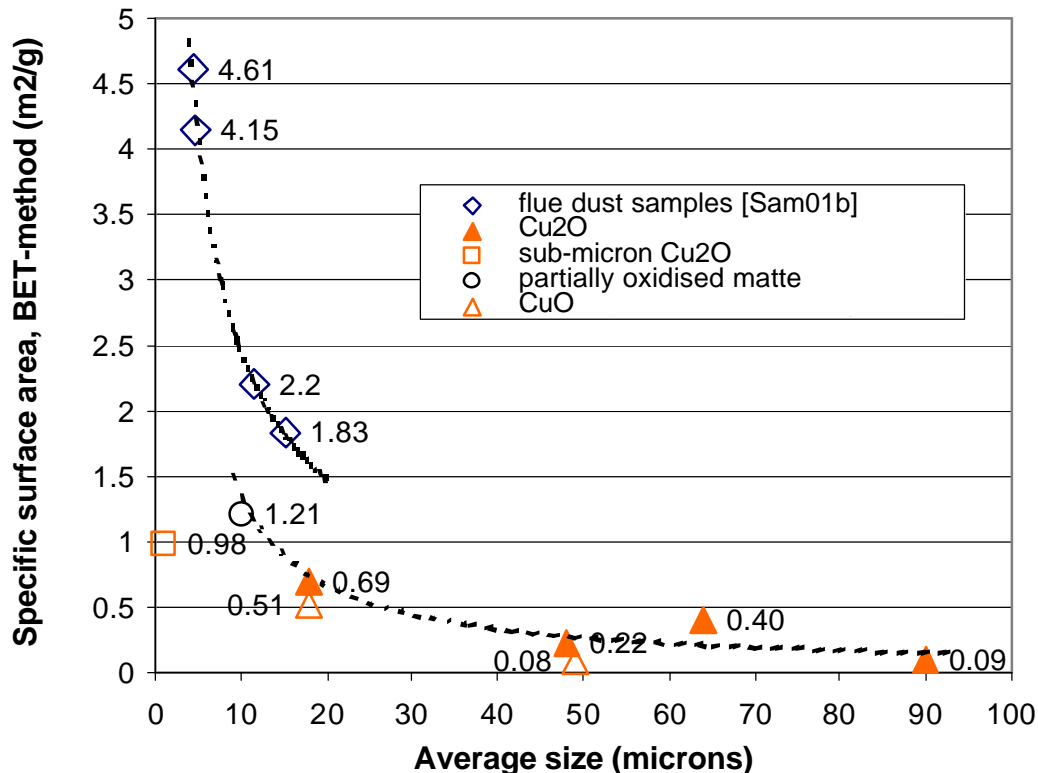
Figure 42. Measured specific surface areas of studied feed materials and process dust [Sam01b]

In the current experiments, none of the samples reached complete conversion. And generally, sulphate amounts did not reach smelter levels. For example, in the case of cuprous oxide (37-53 µm), less than 30 wt-% of $CuSO_4$ was formed at most. There are several reasons for the lower conversion:

- actual process dust is significantly smaller in size and most probably more porous and detailed than the synthetic dusts used in these experiments;

- sulphation is a topochemical reaction in nature and a detailed structure of actual flue dust offers more specific surface area and nucleation points for the reaction;
- incompletely oxidised matte contained relatively many sulphidic particles, presumably more than a typical boiler dust;
- in the current experiments, the particle-gas ratio was slightly different. Typical flue dust loads in the Outokumpu Flash Smelting process range from 100 to 200 g/Nm^3 off-gas *[Isa00]*, while in these experiments the value was approximately 250 g/Nm^3;
- the contribution of the impurities and iron oxides present in the heat recovery boiler dust, and their action as catalyst(s) for SO_3 formation (and thus sulphate formation), were not extensively taken into account here.

4.2 Sulphate formation – thermodynamics

Thermodynamically, both SO_3 and sulphate formation are favoured by low temperatures, but kinetically elevated temperatures generate better outcomes. This yields a maximum formation rate at a certain temperature, which is a compromise between thermodynamics and kinetics. Although SO_3 and sulphate formation are analogous phenomena, the optimal temperature is not the same for both reactions, since sulphate formation includes condensed phases as reactants and products. Thus, the temperature of maximum sulphation is higher than the optimal SO_3 conversion temperature. If oxygen is supplied to too cold region, SO_3 may form but is not consumed by the sulphation reaction. *[Kyt97]*.

Copper has two oxides, cuprous and cupric, the stability of which depends on the prevailing temperature and atmosphere. On the basis of thermodynamic calculations for the Cu-O-S system, $CuSO_4$ is the only stable phase in the conditions studied (Fig. 43). In the case of the Fe-O-S –system, ferric sulphate ($Fe_2(SO_4)_3$) is the stable phase. When both Cu and Fe oxides are present (matte experiments), more stable copper sulphate is assumed to form first. *[Hol70]*

History of the actual process dust is different from what the particles experienced in the current experiments. In the boiler the temperature is not constant, on the contrarily it changes rapidly. The hot particles are rapidly cooled down, and introduced to the temperature range where the sulphates become thermodynamically stable. As can be noticed from Fig. 43, according to the thermodynamics the stable phase at the boiler inlet is Cu_2O. Next CuO turns to be the stable oxide (~ 880-990°C), then oxysulphate (~750-800°C), and finally sulphate (~700-750°C). The gas composition affects the stability temperatures. However, the actual sulphation route can be different. In the XRD analysis of actual FCF and FSF dusts oxysulphate has been found *[Kyt97]*, but the experimental results did not confirm the existence of the oxysulphate.

a)

b)
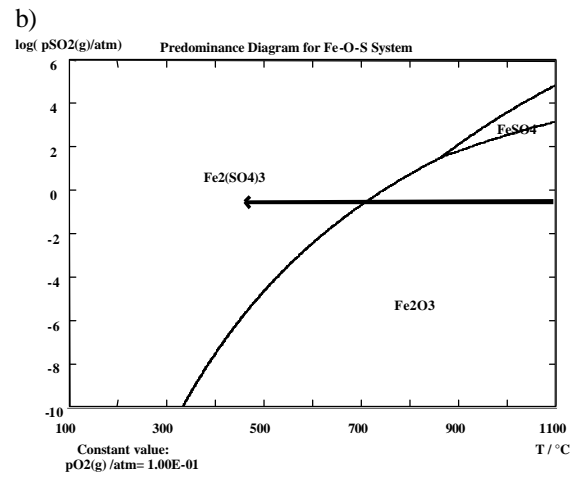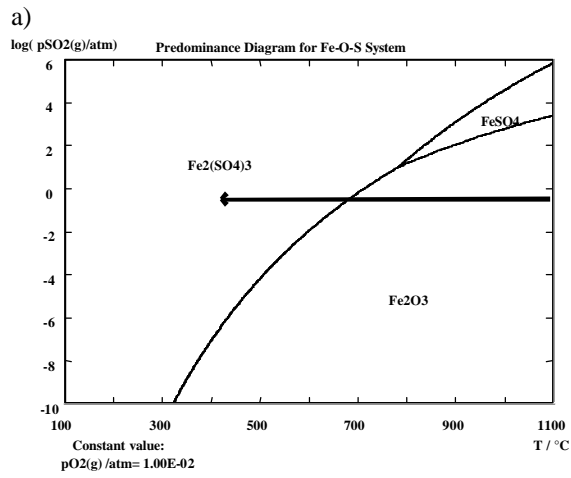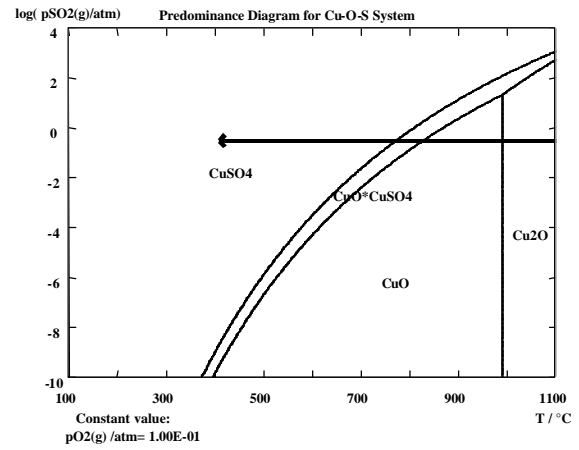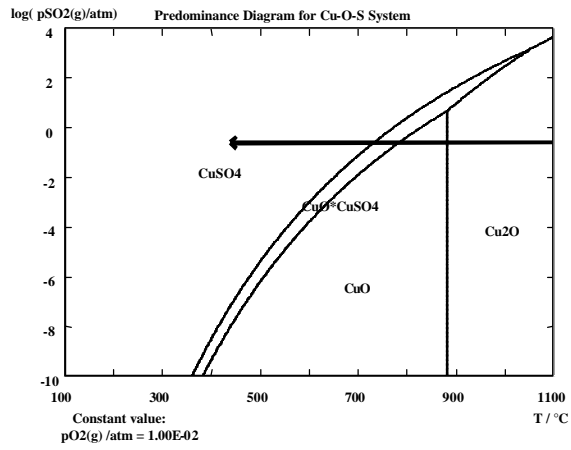
c)

d)

Figure 43. Predominance area diagrams for a-b) Cu-S-O and c-d) Fe-S-O systems calculated using the HSC programme. Oxygen content is constant; a) and c) 1%, b) and d) 10%.

4.3 Effect of oxygen

In the current experiments an increase in oxygen content significantly enhanced sulphate formation, irrespective of the SO_2 partial pressure, temperature, and studied feed material. In the case of cuprous oxide, decreasing the oxygen concentration raises the optimal sulphation temperature. These results are in accordance with SO_3 formation thermodynamics, which are illustrated in Fig. 44. With 2.5 vol-% O_2 the highest temperature for the total conversion is over 600°C, and with 10 vol-% O_2 closer to 500°C than 600°C.

Kinetically, SO_3 formation is slow in the conditions studied, and it is estimated that only 1-3% of sulphur dioxide reacts to sulphur trioxide in the smelter off-gas line *[Sar82]*.

Also, in the experiments the high oxygen concentration expands the favourable temperature range of Cu_2O sulphation.
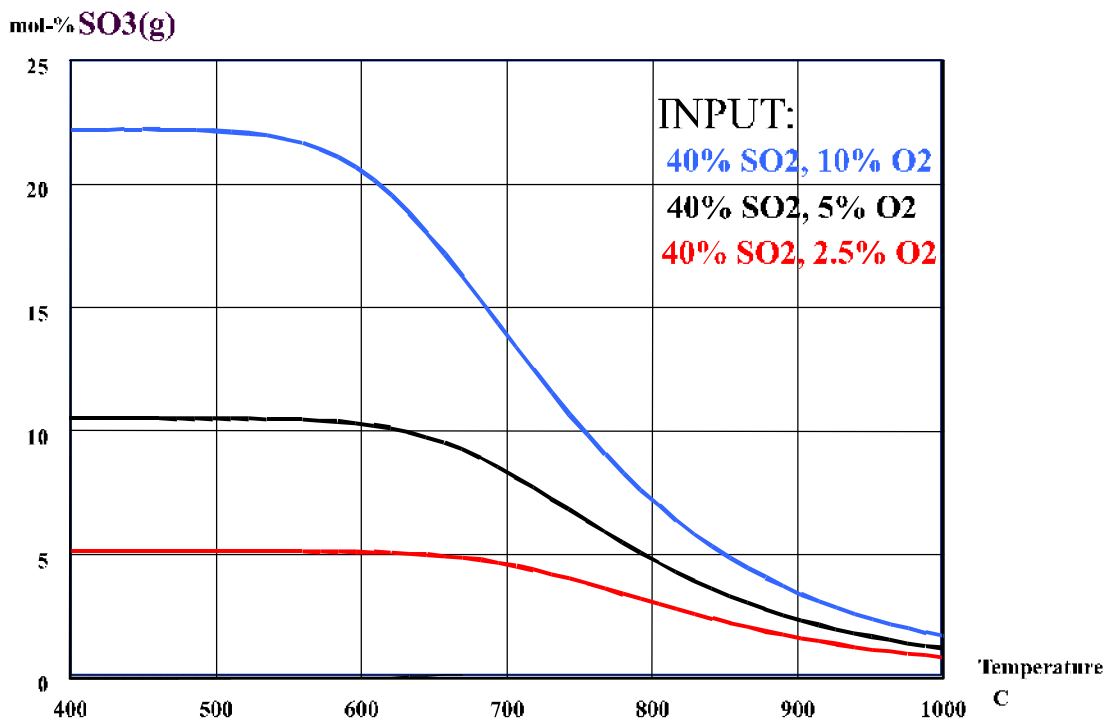
Figure 44. Equilibrium diagram. Effect of oxygen concentration (2.5 – 5 – 10 vol-%) on sulphur trioxide formation thermodynamics. HSC calculation.

4.4 Effect of sulphur dioxide

Experiments with cuprous oxide indicate that increasing the SO_2 content leads to an increase in the temperature of most generous sulphate formation. This is congruent with SO_3 formation behaviour. Fig. 45 presents thermodynamic calculations of SO_3 equilibrium with the used sulphur dioxide contents with constant O_2 (5 vol-%). The lower the SO_2, the lower the maximum temperature for optimal conversion. Unexpectedly, in the current experiments with Cu_2O, a 60 vol-% SO_2 concentration leads to a lower sulphate outcome than 40 vol-%. This might derive from pronounced sintering with higher SO_2.
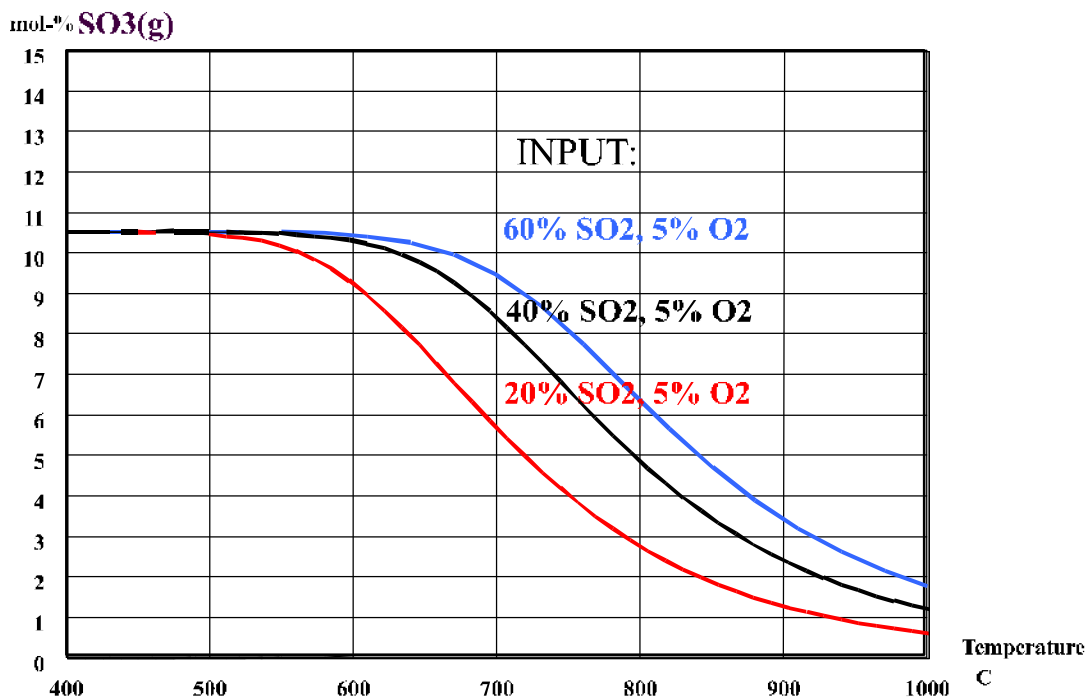
Figure 45. Equilibrium diagram. Effect of sulphur dioxide concentration (20 – 40 – 60 vol-%) on sulphur trioxide formation thermodynamics. HSC calculation.

4.5 Sulphate formation – mechanisms

Sulphate formation is a topochemical reaction starting from the surface and proceeding to the core of the dust particles. Overall sulphation phenomena may be divided into the following steps:

- external mass transfer,
- diffusion through the product layer,
- chemical reaction at the interface.

Heat transfer also has to be taken into account, since sulphate formation is a highly exothermic reaction. The rate-controlling step may change, depending on the conditions; many steps may have more or less equal effects on the overall rate, and the controlling step may change as the reaction proceeds *[Soh79]*.

Pure oxides seemed to be initially nonporous, so the reaction takes place at the sharp interface between the solid and gas phase. As the reaction proceeds a solid (dense) product layer is formed around the initial particles, and constituent species of the solid have to diffuse to the outer surface. If the layer was porous, fluid species could diffuse through the pores of the solid to reach the reaction interface. This dense layer requires solid-state diffusion, and chemical reaction and mass transport are connected in series.

Copper is polyvalent having two different combining powers. A Cu^+ ion needs one negative ion to achieve a stable state, while a Cu^{2+} ion needs two negative ions to form neutral compounds. Thus, cuprous and cupric compounds can be formed. Since the properties and structures (Fig. 46) of CuO and Cu_2O are different, the sulphation behaviour of these oxides is not similar. Cuprous oxide has a structure in which the oxygen ions form a body-centred cubic lattice and each oxygen is tetrahedrally surrounded by four copper ions, and the cations have two nearest oxygen ions. CuO has a structure in which metal ion forms four coplanar bonds. *[Kof72]* Furthermore, molar volume (molecular weight divided by the density) of cuprous oxide is approximately twofold compared to that of cupric oxide (Cu_2O 23.8, CuO 12.6) *[HSC]*
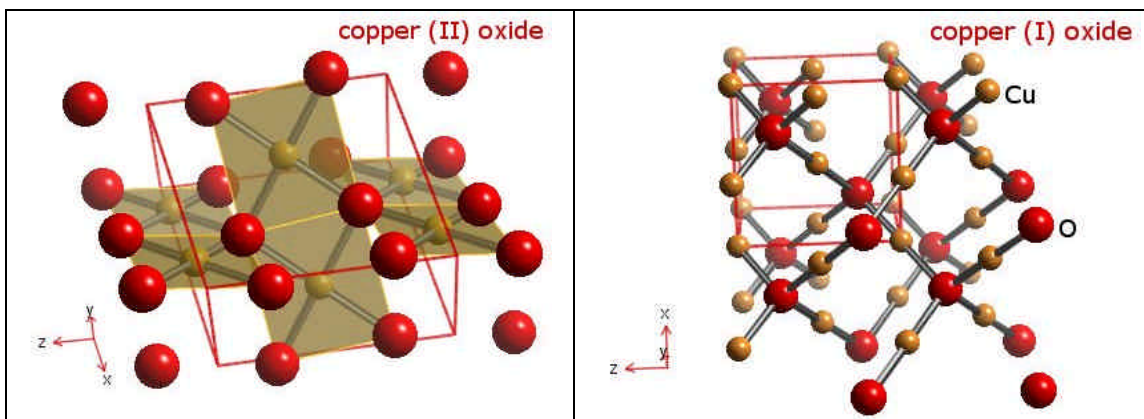
Figure 46. Structures of CuO and Cu_2O [Figures: http://www.webelements.com/]

Cuprous oxide

Direct formation of $CuSO_4$ from Cu_2O is possible, but the reaction can also proceed through the oxy-sulphate phase. Thus, the presence of $CuO \cdot CuSO_4$ in the sulphate layer is possible, depending on the diffusional rates of the species through forming product layers. Direct sulphate formation from cuprous oxide can take place via two reactions,

either reacting directly with oxygen and sulphur dioxide, Eq. (3), or, if sulphur trioxide is present in the atmosphere, reacting with it (Eqs. 4a–b):

$$Cu_2O(s) + 2SO_2(g) + \tfrac{3}{2}O_2(g) = 2CuSO_4(s) \tag{3}$$

$$SO_2(g) + \tfrac{1}{2}O_2(g) = SO_3(g) \tag{4a}$$

$$Cu_2O(s) + 2SO_3(g) + \tfrac{1}{2}O_2(g) = 2CuSO_4(s) \tag{4b}$$

At elevated temperatures the equilibrium conversion amount of SO_2 to SO_3, Eq.(4a), is very small. As off-gas is cooled down the equilibrium amount of SO_3 increases, and below 760°C a rapid conversion of SO_2 to SO_3 can take place if a suitable catalyst is present *[Saf98]*. In heat recovery boiler conditions Eqs. 4a–b apply because catalytic surfaces (copper and iron oxides) for sulphur trioxide formation are generously available.

When Cu_2O particles are completely covered by the sulphate layer, the reaction becomes more complicated. Sulphation could continue in pores and cracks, but, on the basis of the cross-sections studied, sulphate phases seem to be rather dense, and thus reacting species must diffuse through the solid sulphate to the reaction zone. The CuO layer found between the Cu_2O core and the sulphate suggests the outward migration of Cu cations. Loss of copper ions results in the conversion of Cu_2O to CuO. For every migrated copper ion a CuO molecule is formed; also, one molecule of CuO will be left inside, since a copper ion removed from Cu_2O leaves behind a molecule of CuO.

The existence of a CuO layer is supported by the investigations of Hocking and Alcock *[Hoc66]* and Wadsworth et al. *[Wad60]*. Wadsworth et al. sulphated synthetic Cu_2O plates in various mixtures of SO_2 and O_2. Up to 750°C the product layers from the inside to the outer surface were: Cu_2O-CuO-CuO·$CuSO_4$-$CuSO_4$. At 650°C oxy-sulphate (CuO·$CuSO_4$) was partly missing. Above 800°C no sulphates were detected. The reactions followed the parabolic rate law, indicating that diffusion is the rate-controlling factor. The maximum sulphation rate was gained with an SO_2:O_2 ratio of 2:1.

Hocking and Alcock *[Hoc66]* also studied the sulphation of Cu_2O blocks, and showed with gold markers that CuO grows on Cu_2O by the outward migration of copper ions. At 688°C thin oxy-sulphate layer grows by inward migration of sulphating species, which attack the CuO layer, and thick sulphate layer grows outwards from the oxide surface by outward migration of copper ions. At 757°C both very thick oxy-sulphate and thinner sulphate formed by outward diffusion of copper ions from Cu_2O leaving CuO to the core. Their studies supported the same order of product layers as that published by Wadsworth et al *[Wad60]*. Sulphate formation slowed down significantly after total conversion of Cu_2O to CuO. Sulphation reaction rate increased with increasing SO_3 partial pressure. *[Hoc66]* Cu_2O is a metal-deficient oxide with cation vacancies, and the self-diffusion of cations is several orders of magnitude faster than oxygen ion diffusion. Also, the diffusion of copper in CuO is much slower than in Cu_2O *[Kof72/Ani99]*.

In case of Cu_2O sulphation an intermediate layer of CuO was found. Since two molecules of CuO are formed out of one Cu_2O, molar volume of cupric oxide layer is slightly higher than that of the cuprous oxide. On the basis of the molar volume ratio the forming cupric oxide layer should be dense. According to the SEM-studies (Fig. 25b) it appears to be more detailed than the original cuprous oxide surface. The

sulphate layer with even higher molar volume (44.3) forms a dense, protective layer on a particle, and diffusion rate through it is affecting the sulphate formation rate.

The sulphation mechanism for direct sulphation of Cu_2O is illustrated in Figure 47.
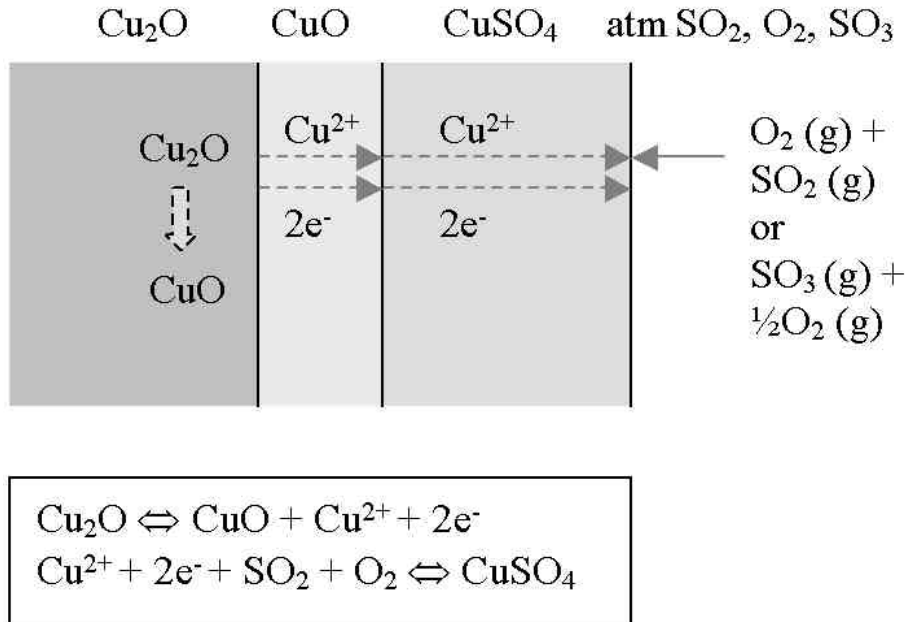
Figure 47. Cu_2O sulphation mechanism. Cations with balancing electrons diffuse through forming CuO and sulphate layer to sulphate/gas interface, where SO_2+O_2 is picked up. CuO is left inside.

Cupric oxide

The presence of either oxygen vacancies or copper interstitials or clusters of them are proposed when the defect structure of cupric oxide is considered. *[Car99]* On the basis of thermodynamic calculations the sulphation of cupric oxide occurs through the oxy-sulphate, according to the following equations:

$$2CuO(s) + SO_3(g) = CuO \cdot CuSO_4 \ (s) \tag{5a}$$

$$CuO \cdot CuSO_4 \ (s) + SO_3(g) = CuSO_4 \ (s) \tag{5b}$$
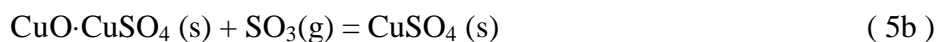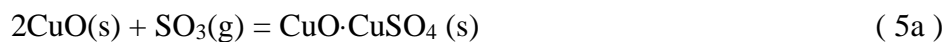
Sulphate formation requires the outward diffusion of Cu^{2+} and O^{2-} ions, or inward diffusion of sulphating species. Sahoo et al *[Sah85]* studied CuO sulphation at temperatures under 600°C. They suggest $CuSO_4$ growth by outward diffusion of Cu^{2+} ions, and formation of oxy-sulphate by a reaction between CuO and $CuSO_4$. Hocking and Alcock *[Hoc66]* propose that at lower temperatures (688°C) oxy-sulphate grows by inward migration of sulphating species.

In the CuO sulphation experiments the intermediate oxy-sulphate layer was not found in the SEM-micrographs. It might be either totally missing, or more presumably mixed with $CuSO_4$, and too thin to be detected. The sulphate layer appears to be dense, and attached to the core oxide, which is supported by that fact that the molar volume of $CuSO_4$ is notably higher than that of CuO. The sulphation mechanism for CuO is illustrated in Figure 48.

$$CuO \quad CuO \cdot CuSO_4 \quad CuSO_4 \quad atm\ SO_2, O_2, SO_3$$

High temperature $\quad Cu^{2+} \quad\quad Cu^{2+} \quad\quad\quad SO_3\ (g)$

$O^{2-} \quad\quad O^{2-}$

Low temperature $\quad Cu^{2+} \quad\quad Cu^{2+} \quad\quad SO_3\ (g)$
$+\tfrac{1}{2}O_2$

$O^{2-} \quad\quad S^{6+}$

$$Cu^{2+} + O^{2-} + SO_3 \Leftrightarrow CuSO_4$$

$$3O^{2-} + S^{6+} + 2\ CuO \Leftrightarrow CuO \cdot CuSO_4$$
$$3Cu^{2+} + 3O^{2-} + 3\ SO_3 \Leftrightarrow 3CuSO_4$$
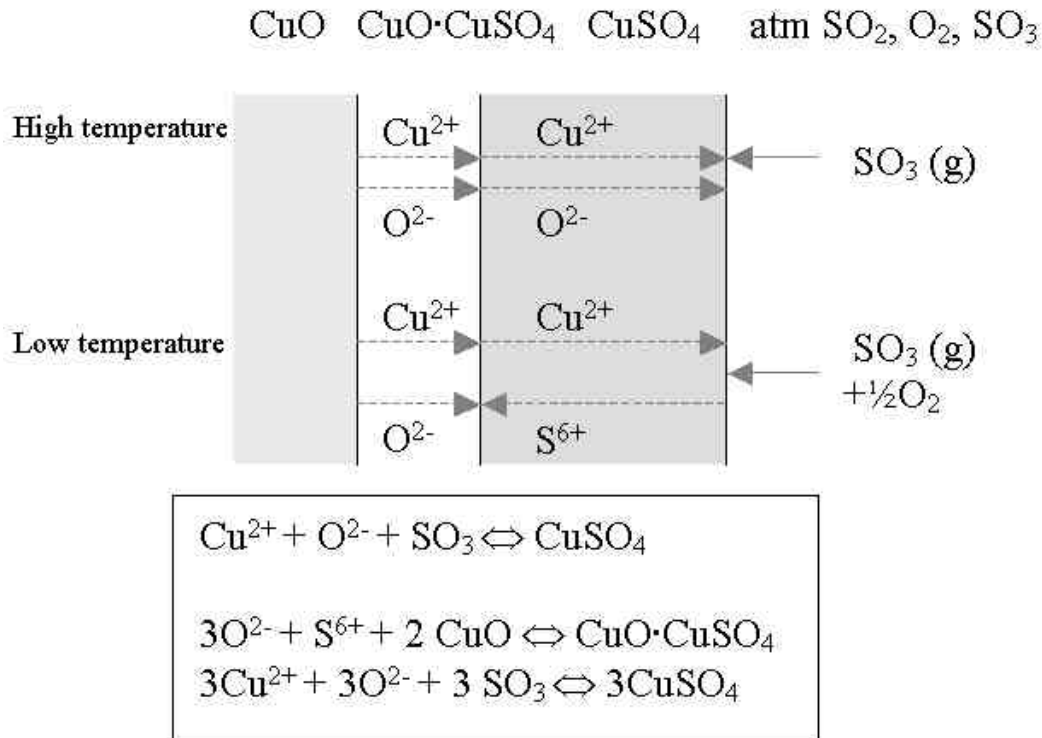
Figure 48. CuO sulphation mechanism. At high temperature (approx. 700 °C) copper and oxygen ion pairs diffuse outwards through sulphate layers. At low temperatures copper sulphate growth results from outward diffusion of copper cations, and oxy-sulphate grows by inward diffusion of sulphating species.[Hoc66]

4.6 Reliability of the results

The used experimental method and equipment are considered to be reliable, since the results are logical, except for a few single data points, and they match with the results of other researchers *[Hoc66, Wad60, Sah85]*.

The most probable source of error in the current results is the inaccuracy of the chemical analyses caused by the inhomogenity of the samples, particularly with partially oxidised matte and sub-micron-sized Cu_2O, and limited sample amounts. However, in general, accuracy of these standard chemical analyses is very good, the relative error is only 2-5%.

Particularly sub-micron-sized Cu_2O tended to agglomerate heavily, and reacted samples were clearly non-homogeneous, which made representative sampling action rather difficult. Also, with the partially oxidised matte the feed was already non-homogeneous and the sample size small. Thus, the slight inconsistency of the few data points and the unexpected decreasing of the sulphation degree as a function of the residence time in these few cases (Figs. 14e, 27, 36, 37) are most probably due to either an inaccuracy in the chemical analysis or human error in the experimental procedure.

5 CONCLUSIONS

Reactions of synthetic Cu_2O and CuO (mainly 37-53 µm) and a partly oxidised copper matte were experimentally studied with the aim of arriving at a better understanding of dust sulphation in industrial HRBs. The parameters in the laboratory-scale experiments were gas composition (20-60 vol-% SO_2, 2.5-10 vol-% O_2), temperature (560-660°C), reaction time, and particle size.

Generally, sulphate amounts did not reach typical smelter levels. 30 wt-% of copper sulphate (from cuprous oxide) was formed at most. The clear reasons for this lower conversion are larger particle size and different surface morphology (smaller specific surface area). The effects of impurities (Na, K) were not studied. Additives may change the optimal sulphation temperature range.

On the basis of the experiments, the following conclusions can be drawn.
- In general:
    - particle size and surface morphology have significant effects on the conversion rate. As expected, a large specific surface area and detailed surface pattern were found to promote conversion;
    - according to the current results, the optimal sulphation temperature depends on the gas composition (O_2, SO_2), and, on the basis of the thermodynamic calculations, is parallel with the optimal SO_3 formation temperature;
    - an increase in oxygen concentration and residence time promotes sulphate formation;
    - on the basis of the current experiments, sintering increases with increasing conversion degree.

- For pure cuprous oxides:
    - in the conditions studied the optimal temperature for sulphation lies between 580-640°C, depending on the gas composition. Before, and, particularly, after the optimal temperature the sulphation rate decreases sharply;
    - the temperature range for effective sulphation is narrow;
    - the present results suggest that an increase in oxygen concentration expands the favourable temperature range and lowers the optimal sulphation temperature;
    - an increase in sulphur dioxide concentration raises the optimal sulphation temperature. With fixed O_2 the optimal temperature is roughly 20°C higher with 40 and 60 vol-% SO_2 compared to 20 vol-%;
    - a high sulphur dioxide concentration (60 vol-%) and long residence time enhance sintering and result in lower conversion compared to experiments with lower sulphur dioxide (40 vol-%);
    - Pt catalyst slightly enhances sulphate formation and lowers the favourable sulphation temperature.

- For pure cupric oxide:
    - generally, cupric oxide behaves like cuprous oxide, but conversion degrees are slightly lower;
    - sulphation of cupric oxide is not equally sensitive to temperature; there is not such a clear enhance in sulphation rate at a certain temperature.

- For partially oxidised matte:

- heterogeneous, fine dust reacts significantly faster right at the beginning compared to synthetic, inert feeds. Smaller size and detailed morphology mean a larger specific surface area and initial points for the reaction.

Implications for the process and equipment

Dust particles must have a sufficient residence time in the gas phase at a correct temperature range to allow the small particles to reach complete conversion. In the case of larger particles, at least the surfaces must be covered by a thick sulphate layer before they enter the convection section and come into contact with the convection tube banks. Otherwise, still-reacting soft particles easily form dust accretions when coming into contact with heat transfer surfaces. Decreased heat transfer efficiency and blockages of the gas flow paths may cause serious operational problems.

Enough oxygen has to be supplied to the appropriate zone to ensure effective sulphation at the right place. If the mixing of the oxygen is efficient, a small amount of oxygen can be adequate.

Future studies

To establish the overall behaviour of flue dust in the boiler, further experimental studies are required. The following topics are suggested:
- the sulphation behaviour of pure iron, zinc, and lead oxide components;
- the sulphation of mixtures, and
- the effects of impurity components (Na, K).

If studies are continued with the current experimental apparatus, an improvement is proposed:
- on-line temperature measurement of the gas-particle suspension to study the potential temperature increase of the suspension caused by the highly exothermic reactions.

REFERENCES

[Ani99]   Aniekwe, U.V., Utigard, T.A., "High-Temperature Oxidation of Nickel-Plated Copper vs Pure Copper", *Canadian Metallurgical Quarterly*, Vol. 38, No. 4, pp. 277-281, 1999.

[Bac86]   Backman, R., Hupa, M., Mäkinen, J.K., "Formation and Corrosion Effects of Sulfur Trioxide in Copper Smelting Processes", The Metallurgical Society of AIME, *TMS Technical Paper No. A86-56, 1986*.

[Bis94]   Biswas, A.K., Davenport, W.G., *Extractive Metallurgy of Copper*, Oxford: Pergamon, 500 p., 1994.

[Bry58]   Bryk, P., Ryselin, J., Honkasalo, J., Malmstrom, R., "Flash Smelting of Copper Concentrates", *J. Met.*, Vol. 10 June, pp. 395-400, 1958.

[Car99]   Carel, C., Mouallem-Bahout, M., Gaudé, J., "Re-examination of the non-stoichiometry and defect structure of copper(II) oxide or tenorite, $Cu_{1\pm z}O$ or $CuO_{1\pm \in}$ A short review", *Solid State Ionics*, Vol. 117, pp. 47-55, 1999.

[Dav87]   Davenport W.G., Partelpoeg E.H., *Flash Smelting: Analysis, Control and Optimisation*, Oxford: Pergamon, 324 p., 1987.

[Gre67]   Gregg, S.J., Sing, K.S.W., *Adsorption, Surface Area and Porosity*, Academic Press, London, 1967, 371 p.

[Han98]   Hanniala P., Kojo I.V., Kytö M., "Kennecott-Outokumpu Flash Converting Process – Copper by Clean Technology", In: Asteljoki J.A., Stephens R.L., (eds.), *Sulfide Smelting '98 – Current and Future Practices*, Minerals, Metals and Materials Society of the AIME, Warrendale, PA, USA, pp. 239-247, 1998.

[Hoc66]   Hocking M.G., Alcock C.B., "The Kinetics and Mechanism of Formation of Sulfates on Cuprous Oxide", *Transactions of the Metallurgical Society of AIME*, 236, pp. 635-642, 1966.

[Hol70]   Holappa, L.E.K., "Kinetics and Mechanism of Sulphation of Cobalt and Nickel Oxides", *Acta Polytechnica Scandinavica – Chemistry Including Metallurgy Series*, No. 92, 57 p., 1970.

[Isa00]   Isaksson Ö., Lehner T., "The Rönnskär Smelter Project: Production, Expansion, and Start-up", *JOM*, Vol. 52, No. 8, pp. 26-29, 2000.

[Jon96]   Jones D.M., and Davenport W.G., "Minimization of Dust Generation in Outokumpu Flash Smelting", In: Warren, G., (ed.), *EPD Congress 1996*, Minerals, Metals and Materials Society of the AIME, Warrendale, PA, USA, pp. 81-94, 1996.

[Kof72]   Kofstad, P., *Nonstoichiometry, Diffusion, and Electrical Conductivity in Binary Metal Oxides*, John Wiley & Sons, Inc., New York, 1972, 382 p.

[Kyt97]   Kytö M., Private Communication, 2 April 1997. "Theoretical Aspects on Flash Converting and Direct Blister Copper Production", *The 7th International Flash Smelting Congress, 25-28.10.1993, Korea*. and manuscript for the presentation "Mineralogical Characterization of Copper Flash Converting Flue Dusts" at 121st *TMS Annual Meeting 2-5.3.1992 in San Diego*.

[Liu03]   Liu J., Warner, A.E.M., Osborne, G., Cooke, D., Slayer, R., "The Operation of INCO Flash Furnace Uptake: Combustion of H_2S and formation of uptake buildup". In: Kongoli F., Itagaki K., Yamauchi, C., Sohn H.Y. (eds.), High-Temperature Metal Production. *Proceedings of Yazawa International Symposium.* TMS, pp. 143-152, 2003.

[Low91]   Lowell, S., Shields, J.E., *Powder Surface Area and Porosity*, 3rd edition, Chapman&Hall, London, 1991, 250 p.

[Mar00]   Markova, Ts., Boyanov, B., Pironkov, S., Shopov, N., "Investigation of Dusts From Waste-Heat Boiler and Electrostatic Precipitators After Flash Smelting Furnace for Copper Concentrates", *J.Min.Met.* vol. 36 No. 3-4B, pp. 195-208, 2000.

[Pel01]   Peltola, H., Outokumpu Research Oy, Private communication. Internal report 01047-ORC-T. 2001.

[Peu99]   Peuraniemi, E., Järvi, J., Jokilaakso, A., "Behaviour of Copper Matte Particles in Suspension Oxidation", In: Díaz C., Landolt C., Utigard, T. (eds.),. *Copper 99 – Cobre 99 - Vol. VI Smelting, Technology Development, Process Modeling and Fundamentals*, TMS (Minerals, Metals & Materials Society), Phoenix, Arizona, USA, pp. 463-473, 1999.

[Peu00]   Peuraniemi, E., Jokilaakso, A., Laminar flow furnace in flash oxidation experiments of copper concentrate (in Finnish), *Helsinki University of Technology Publication in Materials Science and Metallurgy*; Report TKK-MK-96, 30 p., 2000.

[Peu01]   Peuraniemi, E.J., Saarikoski, A., Ranki-Kilpinen, T., "Behaviour of Cu_2O Particles in Copper Smelting Heat Recovery Boiler Conditions", In: Taylor, P.R. (ed.), *EPD Congress 2001*, TMS (Minerals, Metals & Materials Society), New Orleans, Louisana, USA, pp. 421-430, 2001.

[Ran00]   Ranki-Kilpinen T., Peuraniemi E., Jokilaakso A., "Sulphation of Synthetic Flue Dust Particles in SO_2-O_2-N_2 Atmosphere". In: G. Kaiura, C. Pickles, T. Utigard, A. Vahed (eds.), Fundamentals of Metallurgical Processing. *Proceedings of James M. Toguri Symposium.* CIM, pp. 193-206, 2000.

REFERENCES

[Ran02]	Ranki-Kilpinen T., Peuraniemi E., Mäkinen, M., "Sulphation of Cuprous Oxide in SO_2-rich Atmospheres", In: Stephens R.L., Sohn, H.Y., (eds.), *Sulfide Smelting 2002*, The Minerals, Metals & Materials Society, Warrendale, USA, pp. 261-271, 2002.
[Saf98]	Safe P., Jones D.M., "Process Off-gas Cooling Design Considerations for Non-ferrous Metallurgical Processes", In: Asteljoki J.A., Stephens R.L., (eds.), *Sulfide Smelting '98 – Current and Future Practices*, Minerals, Metals and Materials Society of the AIME, Warrendale, PA, USA, pp. 401-415, 1998.
[Sah84a]	Sahoo P.K., Sircar S.C., Bose S.K., "Studies in Sulphation: 1 – Kinetics and Mechanism of Sulphation of Manganese Dioxides", *Transactions/ Institution of Mining and Metallurgy. Section. C, Mineral Processing & Extractive Metallurgy*, Vol. 93, No. C9-C13, 1984.
[Sah84b]	Sahoo P.K., Sircar S.C., Bose S.K., "Studies in Sulphation: 2 – Sulphation of Fe_2O_3 and Manganese Ore in SO_2-O_2 Atmospheres", *Transactions/ Institution of Mining and Metallurgy. Section. C, Mineral Processing & Extractive Metallurgy*, Vol. 93, No. C13-C15, 1984.
[Sah85]	Sahoo P.K., Sircar S.C., Bose S.K., "Studies in Sulphation: 3 – Kinetics and Mechanism of Sulphation of Cupric Oxides", *Transactions/ Institution of Mining and Metallurgy. Section. C, Mineral Processing & Extractive Metallurgy*, Vol. 94, No. C1-C3, 1985.
[Sam98]	Samuelsson, C., Björkman, B., "Dust Forming Mechanisms in the Gas Cleaning System After the Copper Converting Process, *Scandinavian Journal of Metallurgy*, Vol. 27, pp. 64-72, 1998.
[Sam01a]	Samuelsson, C., Carlsson, G., "Characterization of Copper Smelter Dusts", *CIM Bulletin*, Vol. 94, No 1051, pp. 111-115, 2001.
[Sam01b]	Samuelsson, C., Carlsson, G., "A Qualitative Study on the Retention of Mercury from SO_2-containing Process Gases on Copper Smelter Dusts, *Canadian Metallurgical Quaterly*, Vol. 40, No 2, pp. 161-168, 2001.
[Sar82]	Sarkar, S., "Effect of SO_3 on Corrosion of Process Equipment in Copper Smelters", *JOM*, vol. 34, Oct., pp. 43-47, 1982.
[Soh79]	Sohn, H. Y., Wadsworth, M. E. (eds.), *Rate Processes of Extractive Metallurgy*, Plenum Press, New York, 472 p., 1979.
[StE94]	St. Eloi, R.J., Newman, C.J., Macfarlane, G., "Modifications to the Process Gas Handling system at Kidd Creek's Copper Smelter", *CIM Bulletin*, Vol. 87, No. 977, pp. 77-85, 1994.

[Swi02]   Swinbourne, D.R., Simak, E., Yazawa, A., "Accretion and Dust Formation in Copper Smelting – Thermodynamic Considerations", In: Stephens, R.L. and Sohn, H.Y. (eds.), *Sulfide Smelting 2002*, TMS (Minerals, Metals & Materials Society), Seattle, Washington, USA, pp. 247-259, 2002.

[Tas02]   Taskinen, P., Private Communication, 2002.

[Wad60]   Wadsworth M.E., Leiter K.L., Porter W.H., Lewis J.R., "Sulfating of Cuprous Sulfide and Cuprous Oxide", *Transactions of the Metallurgical Society of AIME*, Vol. 218, pp. 519-525, 1960.

[Yan96]   Yang, Y., "Computer Simulation of Gas Flow and Heat Transfer in Waste-Heat Boilers of the Outokumpu Copper Flash Smelting Process", *Acta Polytechnica Scandinavica - Chemical Technology Series*, No. 242, 135 p., 1996.

[Yan97]   Yang, Y., Jokilaakso, A., Thermodynamic Analysis of Dust Sulphation Reactions, *Helsinki University of Technology Publication in Materials Science and Metallurgy*; Report TKK-MK-27, 29 p., 1997.

[HSC]   HCS Chemistry for Windows, ver. 5.1 Outokumpu Research Oy.

APPENDIX A

CHEMICAL ANALYSES

<u>Synthetic Cu$_2$O</u>

Preliminary experiments

Synthetic Cu$_2$O Fraction 74-105 μm				LECO	IC
T	O$_2$	SO$_2$	t	S	SO$_4$
(^{o}C)	(vol-%)	(vol-%)	(s)	(%)	(%)
500	40	20	60	1.1	
500	40	20	80	1.6	
500	40	20	120	1.9	
600	40	20	60	1.4	
600	40	20	80	1.7	
600	40	20	120	1.7	5.1
650	40	20	60	1.8	5.5
650	40	20	80	2.0	
650	40	20	120	2.3	7.3
700	40	20	60	0.2	
700	40	20	80	0.3	
700	40	20	120	0.4	

Particle size and Pt catalyst

Synthetic Cu$_2$O Fraction 37-53 μm					LECO
	T	O$_2$	SO$_2$	t	S
	(^{o}C)	(vol-%)	(vol-%)	(s)	(%)
75-105 µm	600	5	40	60	0.69
53-75 µm	600	5	40	60	1.1
-37 µm	600	5	40	60	5.4
Pt	640	5	40	60	1.3
Pt	600	5	40	60	2.8
Pt	580	5	40	60	2.1
Pt	620	5	40	60	2.0

Synthetic Cu$_2$O Fraction 37-53 μm				LECO		Synthetic Cu$_2$O Fraction 37-53 μm				LECO
T	O$_2$	SO$_2$	t	S		T	O$_2$	SO$_2$	t	S
(^{o}C)	(vol-%)	(vol-%)	(s)	(%)		(^{o}C)	(vol-%)	(vol-%)	(s)	(%)
560	10	20	120	4.6		640	2.5	20	120	1.40
560	10	20	80	4.3		640	2.5	20	80	0.74
560	10	20	60	2.6		640	2.5	20	60	0.41
560	10	20	40	1.4		640	2.5	20	40	0.24
560	10	20	20	1.3		640	2.5	20	20	0.03
580	2.5	20	120	1.3		640	5	20	120	2.5
580	2.5	20	80	0.92		640	5	20	80	1.3
580	2.5	20	60	0.62		640	5	20	60	1.0
580	2.5	20	40	0.82		640	5	20	40	0.39
580	2.5	20	20	0.37		640	5	20	20	0.1
580	5	20	120	2.5		640	10	20	120	3.8
580	5	20	80	2.0		640	10	20	80	3.1
580	5	20	60	1.6		640	10	20	60	2.2
580	5	20	40	1.3		640	10	20	40	0.66
580	5	20	20	0.54		640	10	20	20	0.25
580	10	20	120	4.9		660	2.5	20	120	1.2
580	10	20	80	4.5		660	2.5	20	80	0.15
580	10	20	60	2.6		660	2.5	20	60	0.07
580	10	20	40	1.8		660	2.5	20	40	0.02
580	10	20	20	1.1		660	2.5	20	20	0.01
600	2.5	20	120	1.4		660	5	20	120	1.6
600	2.5	20	80	1.6		660	5	20	80	0.56
600	2.5	20	60	1.3		660	5	20	60	0.24
600	2.5	20	40	0.51		660	5	20	40	0.18
600	2.5	20	20	0.20		660	5	20	20	0.01
600	5	20	120	3.3		660	10	20	120	1.9
600	5	20	80	3.1		660	10	20	80	0.60
600	5	20	60	2.3		660	10	20	60	0.28
600	5	20	40	1.4		660	10	20	40	0.02
600	5	20	20	0.5		660	10	20	20	0.01
600	10	20	120	4.7						
600	10	20	80	3.6						
600	10	20	60	3.4						
600	10	20	40	1.8						
600	10	20	20	0.71						
620	2.5	20	120	2.7						
620	2.5	20	80	1.8						
620	2.5	20	60	1.4						
620	2.5	20	40	0.81						
620	2.5	20	20	0.22						
620	5	20	120	3.8						
620	5	20	80	2.0						
620	5	20	60	1.6						
620	5	20	40	1.0						
620	5	20	20	0.55						
620	10	20	120	4.3						
620	10	20	80	3.4						
620	10	20	60	2.6						
620	10	20	40	1.4						
620	10	20	20	0.37						

Synthetic Cu$_2$O Fraction 37-53 μm				LECO	Synthetic Cu$_2$O Fraction 37-53 μm				IC
T	O$_2$	SO$_2$	t	S	T	O$_2$	SO$_2$	t	SO$_4$
(^{o}C)	(vol-%)	(vol-%)	(s)	(%)	(^{o}C)	(vol-%)	(vol-%)	(s)	(%)
600	2.5	40	120	1.6	640	2.5	40	120	6.1
600	2.5	40	80	1.1	640	2.5	40	80	4.6
600	2.5	40	60	0.96	640	2.5	40	60	3.8
600	2.5	40	40	0.71	640	2.5	40	40	1.7
600	2.5	40	20	0.37	640	2.5	40	20	1.2
600	5	40	120	3.3	640	5	40	120	10.9
600	5	40	80	2.4	640	5	40	80	8.8
600	5	40	60	1.6	640	5	40	60	3.2
600	5	40	40	1.3	640	5	40	40	2.5
600	5	40	20	0.56	640	5	40	20	1.5
600	10	40	120	5.6	660	2.5	40	120	4.5
600	10	40	80	2.8	660	2.5	40	80	2.1
600	10	40	60	3.0	660	2.5	40	60	2.2
600	10	40	40	1.7	660	2.5	40	40	2.7
600	10	40	20	1.3	660	2.5	40	20	0.5
620	2.5	40	120	2.3	660	5	40	120	4.4
620	2.5	40	80	1.8	660	5	40	80	5.1
620	2.5	40	60	1.2	660	5	40	60	4.1
620	2.5	40	40	0.65	660	5	40	40	2.9
620	2.5	40	20	0.35	660	5	40	20	2.5
620	5	40	120	4.0					
620	5	40	80	3.5					
620	5	40	60	2.5					
620	5	40	40	2.3					
620	5	40	20	1.2					
620	10	40	120	4.4					
620	10	40	80	4.1					
620	10	40	60	3.5					
620	10	40	40	3.0					
620	10	40	20	2.5					

Synthetic Cu₂O Fraction 37-53 μm				LECO	IC
T	O₂	SO₂	t	S	SO₄
(°C)	(vol-%)	(vol-%)	(s)	(%)	(%)
600	2.5	60	120	1.1	4.22
600	2.5	60	80	1.0	3.18
600	2.5	60	60	0.9	2.85
600	2.5	60	40	0.7	2.28
600	2.5	60	20	0.4	1.51
600	5	60	120	2.1	7.66
600	5	60	80	1.3	4.42
600	5	60	60	1.2	3.64
600	5	60	40	0.6	2
600	5	60	20	0.4	1.3
620	2.5	60	120		5.4
620	2.5	60	80		5.1
620	2.5	60	60		2.9
620	2.5	60	40		2.9
620	2.5	60	20		0.8
620	5	60	120		12.1
620	5	60	80		6.1
620	5	60	60		7.5
620	5	60	40		3.9
620	5	60	20		1.4
640	5	60	120	1.9	5.1
640	5	60	80	1.5	5
640	5	60	60	1.5	3.8
640	5	60	40	0.8	3
640	5	60	20	0.5	1.6
640	2.5	60	120	1.8	4.8
640	2.5	60	80	1.0	2.2
640	2.5	60	60	0.6	2.1
640	2.5	60	40	0.8	2.1
640	2.5	60	20	0.2	0.86
660	2.5	60	120	1.0	3.9
660	2.5	60	80	1.6	3.1
660	2.5	60	60	0.7	1.9
660	2.5	60	40	0.4	1.6
660	2.5	60	20	0.2	0.77
660	5	60	120	2.3	6.1
660	5	60	80	2.0	6.2
660	5	60	60	1.3	4.2
660	5	60	40	1.0	3.1
660	5	60	20	0.6	1.5

Synthetic sub-micron Cu_2O				LECO	IC
T	O_2	SO_2	t	S	SO_4
(°C)	(vol-%)	(vol-%)	(s)	(%)	(%)
580	5	20	10	0.60	1.7
580	5	20	20	0.87	2.5
580	5	20	40	1.5	4.9
580	5	20	60	4.0	12.4
580	5	20	120	3.7	13.0
580	5	20	180	6.5	19.9
600	5	20	10	0.41	1.5
600	5	20	20	0.85	2.8
600	5	20	40	1.7	5.0
600	5	20	60	2.2	6.7
600	5	20	120	3.4	10.7
600	5	20	180	5.5	13.6
620	5	20	10	0.29	0.9
620	5	20	20	0.90	2.9
620	5	20	40	1.3	4.1
620	5	20	60	3.8	10.7
620	5	20	120	5.4	13.5
620	5	20	180	5.7	18.1
640	5	20	10	0.18	0.5
640	5	20	20	0.37	1.1
640	5	20	40	0.97	2.3
640	5	20	60	1.7	5.1
640	5	20	120	2.4	7.7
640	5	20	180	3.8	11.7
660	5	20	10	0.07	0.3
660	5	20	20	0.24	0.6
660	5	20	40	0.37	0.9
660	5	20	60	2.3	6.8
660	5	20	120	2.8	6.9
660	5	20	180	3.7	10.6

				LECO	IC
T	O_2	SO_2	t	S	SO_4
(°C)	(vol-%)	(vol-%)	(s)	(%)	(%)

Synthetic CuO

Synthetic CuO Fraction 37-53 μm				LECO	IC
T	O_2	SO_2	t	S	SO_4
(^{o}C)	(vol-%)	(vol-%)	(s)	(%)	(%)
580	5	40	120	2.5	7.7
580	5	40	60	1.4	4.2
580	5	40	20	0.7	1.5
580	2.5	40	120	1.0	3.0
580	2.5	40	60	0.6	1.7
580	2.5	40	20	0.3	0.9
600	5	40	120	2.6	7.4
600	5	40	60	1.8	5.0
600	5	40	20	0.63	2.0
600	2.5	40	120	1.8	4.9
600	2.5	40	60	0.82	2.5
600	2.5	40	20	0.41	1.0
620	5	40	240	4.8	11.8
620	5	40	180	4.2	10.2
620	5	40	120	2.7	8.4
620	5	40	80	1.7	5.7
620	5	40	60	1.8	5.3
620	5	40	40	1.0	3.0
620	5	40	20	0.9	2.2
620	5	40	10	0.5	1.1
620	2.5	40	120	1.7	5.9
620	2.5	40	80	1.2	3.7
620	2.5	40	60	1.2	3.3
620	2.5	40	40	0.80	2.2
620	2.5	40	20	0.47	0.97
640	5	40	120	2.3	7.7
640	5	40	60	1.6	4.8
640	5	40	20	0.76	1.8
640	2.5	40	120	1.9	5.5
640	2.5	40	60	1.1	3.2
640	2.5	40	20	0.4	1.0
660	5	40	120	3.1	7.3
660	5	40	60	1.6	4.1
660	5	40	20	0.6	1.7
660	2.5	40	120	1.5	4.0
660	2.5	40	60	0.7	1.6
660	2.5	40	20	0.2	0.5
580	5	20	60	1.0	3.1
600	5	20	60	0.9	2.8
620	5	20	60	1.0	3.0
640	5	20	60	0.9	2.6
660	5	20	60	0.4	1.5

Partially oxidised matte

Partially oxidised matte				LECO	IC	ICP	ICP
T	O$_2$	SO$_2$	t	S	SO$_4$	Cu	Fe
(°C)	(vol-%)	(vol-%)	(s)	(%)	(%)	(%)	(%)
560	5	40	120	7.0	13.4	64.6	6.8
560	5	40	60	6.5	11.0	67.2	7.1
560	5	40	20	5.4	6.4	68.4	7.3
560	5	40	10	5.7	5.9	68.9	7.3
580	5	40	120	7.1	12.6	61.7	6.7
580	5	40	60	6.1	8.4	64.0	6.9
580	5	40	20	5.8	6.6	65.0	7.4
580	5	40	10	5.9	5.9	69.2	7.3
600	5	40	120	6.5	8.5	60.6	6.8
600	5	40	60	5.5	9.9	59.7	6.6
600	5	40	20	5.5	7.0	61.5	6.9
620	5	40	120	6.1	8.7	61.0	7.3
620	5	40	60	5.4	6.5	63.8	7.4
620	5	40	20	5.7	5.9	63.1	7.3
640	5	40	120	5.5	7.8	59.5	7.0
640	5	40	60	5.2	6.1	61.4	6.9
640	5	40	20	5.1	6.3	61.0	7.0